1-27-2022

Measurement of Binding Affinity and Receptor Activation of a Novel Curcumin Analog, Cis-Trans Curcumin, at Adenosine Receptors A1, A2A, A2B, and A3

Luke James Hamilton
University of Nebraska at Kearney, hamilton.luke.james@gmail.com

MEASUREMENT OF BINDING AFFINITY AND RECEPTOR ACTIVATION OF A NOVEL CURCUMIN ANALOG, *CIS-TRANS* CURCUMIN, AT ADENOSINE RECEPTORS A_1, A_{2A}, A_{2B}, AND A_3

A Thesis
Presented to the
Graduate Faculty of the Biology Department
and the
Faculty of the Graduate College
University of Nebraska

In Partial Fulfillment
of the Requirements for the Degree
Master of Science
University of Nebraska at Kearney

By
Luke James Hamilton
December 2021

THESIS ACCEPTANCE

Acceptance for the faculty of the Graduate College, University of Nebraska, in partial fulfillment of the requirements for the degree Master of Science, University of Nebraska at Kearney.

Supervisory Committee

Name	Department
[signature]	UNK Chemistry
[signature]	UNK Biology
[signature]	UNK Biology

Surabhi Chandra
Supervisory Committee Chair

12/01/2021
Date

ACKNOWLEDGEMENTS

How can I begin to thank my mentor, Dr. Surabhi Chandra, for her efforts over the past three years? I suppose I'll start with the basics. One of the roles of a research mentor is to help the student learn the techniques necessary to accomplish the work, like how to culture cells or optimize a protocol. In all these details, Dr. Chandra was a thorough and patient teacher. But science, of course, is more than techniques—it is an art. How does one formulate a hypothesis? How does one interpret data? How does one write manuscripts and create presentations to communicate findings? On all these questions and more, I am thankful to Dr. Chandra for sharing her expertise. Dr. Chandra also made time to help me develop as a professional. The field of biomedical science is complicated these days, a labyrinth of industrial, academic, and clinical jobs. I spent quite a bit of time during this master's program reading and thinking about my potential future amid that complicated field, and throughout that process Dr. Chandra was a valuable guide, giving her perspective from years spent working in different places, and encouraging me to aim for my dreams. Finally, and most impactfully, Dr. Chandra helped me to develop my character. Over the past three years I faced a series of personal challenges that frequently overwhelmed me, and that inevitably affected my work. In handling this, Dr. Chandra struck a remarkable balance. She was exceedingly merciful toward all my missed deadlines and other failings, yet at the same time was always there to give me a push when I needed one. Even when I was at my lowest, she encouraged me that I still had potential and that I should try again. She thus taught me the importance of resilience and hope, and for that, I will never be able to thank her enough.

I am also grateful to Dr. Mahesh Pattabiraman. On the practical side, I want to acknowledge him as the originator of the idea for this project, and also as the one who performed the chemical synthesis of our compound of interest, CTCUR. Beyond that, I want to thank him for all the good times we had discussing chemistry, science in general, veganism, and politics. In all these conversations, what struck me most is that Dr. Pattabiraman is the most intellectually humble scientist I know. Never before have I spoken with someone who can in one breath so brilliantly articulate the amazing things that science can do, then with the very next breath express such a profound appreciation of the limits of science and of the possibility that "established" or "textbook" thinking might be wrong. Such intellectual honesty is inspiring, and I am grateful to Dr. Pattabiraman for helping me to develop this same honesty in my own thinking.

Many thanks go to the members of my supervisory committee, Dr. Kimberly Carlson, Dr. Allen Thomas, and Dr. Nicholas Hobbs. This project turned out well in the end, and that is largely because of the advice that they gave when I was designing the project, helping me to choose a hypothesis that I could reasonably test with the time and resources that I had available. They also helped me to become a better writer through their editing of this manuscript. Finally, I am grateful to them for their words of encouragement throughout the project, which helped keep me going.

This project could not have been accomplished without the efforts of those who helped with data collection. Acknowledgement goes to Dr. Haizhen Andy Zhong and Chase Stebbing of the University of Nebraska at Omaha for performing the docking studies, to Dr. Brandon Luedtke for teaching me how to operate the confocal microscope,

to Michaela Walker and Hilary Vaughn for performing the cytotoxicity assays, and to Mary Fiala for helping with the optimization and validation of the competitive binding assay procedure. Your attention to detail and clear communication were very much appreciated!

I am grateful to Betty Jacques, Dr. Paul Twigg, and Luke Fennessy for the great experience I had as a teaching assistant during this master's program. I am grateful to my fellow graduate student Hadassha Tofilau along with all the other UNK Biology graduate students and all the undergraduates of the Chandra lab for being excellent co-workers and friends. I am also deeply grateful to my priest Fr. Christopher Morris, my godfather Levi Hadley, my siblings Bethia and Levi Hamilton, and my friends Eleni McClure and Blase Rokusek for their tireless support during all the adventures of the past three years.

In closing, I would like to dedicate this work to my parents, Roger and Cheryl Hamilton. Their encouragement of my love for birds is what eventually led me to choose biology as my field of study, and their teaching that I should seek to serve the needs of other people is what led me to study biomedicine. Thank you, Mom and Dad, for loving me unconditionally, and for encouraging me to use my talents to serve God and others.

FUNDING ACKNOWLEDGMENTS

This work was supported by the Great Plains IDeA CTR program (NIGMS # 1U54GM115458-01, Chandra and Pattabiraman) and the American Chemical Society Petroleum Research Fund (# 54862-UR4, Pattabiraman). Cell culture facility and fluorescence microscopy facilities at UNK were supported by grants from the National Institute for General Medical Science (NIGMS) (5P20GM103427), a component of the National Institutes of Health (NIH), as well as Nebraska Research Initiative. The Nebraska INBRE program also provided funding support.

ABSTRACT

Vanilloid phytochemicals (VPs), which contain the 4-hydroxy-3-methoxybenzyl group, have consistently been shown to alleviate pain. All four of the adenosine receptor (AR) subtypes mediate pain and have been targeted by pharmacologists to generate new therapeutics for pain. However, despite the fact that both VPs and ARs are connected to pain relief, only a few studies have described the interaction between VPs and ARs. Furthermore, the few studies that have been done have all been performed *in vivo*, with no assessment of binding affinity and receptor activation *in vitro*. In this study, photochemical methods were used to generate a novel isomer of curcumin called *cis-trans* curcumin (CTCUR), and the interactions of CTCUR with each of the four AR subtypes were measured. Cell survival assays were performed to measure toxicity. Competitive binding assays, confocal fluorescence microscopy, and docking analysis were performed to measure binding affinity. Finally, cAMP immunoassays were performed to measure receptor activation. Binding assay results indicated that CTCUR has K_i values of 306 nM, 400 nM, 5,107 nM, and 6,722 nM at AR subtypes A_1, A_3, A_{2A}, and A_{2B}, respectively. These values suggest that CTCUR is selective for G_i-linked ARs over G_s-linked ARs. Docking studies likewise indicated that CTCUR interacts more strongly with the G_i-linked subtypes. Data from cAMP immunoassays at all four subtypes suggest that CTCUR is an agonist of ARs. Docking indicated that CTCUR binds to the toggle switch domain of ARs, which likewise suggests agonistic activity. Thus, this study provides the first *in vitro* and *in silico* data that support the hypothesis that ARs may serve as a mechanism of action for the antinociceptive effect of VPs.

TABLE OF CONTENTS

TABLE OF FIGURES

ABBREVIATIONS

AR, adenosine receptor; cAMP, cyclic adenosine monophosphate; CBA, competitive binding assay; CHO, Chinese hamster ovary; CMGV, corrected mean gray value; CNS, central nervous system; CUR, curcumin; COX, cyclooxygenase; CTCUR, *cis-trans* curcumin; G_i, inhibitory G protein; G_s, stimulatory G protein; GPCR, G-protein-coupled receptor; NECA, 5'-*N*-ethylcarboxamidoadenosine; HEK, human embryonic kidney; MOE, molecular operating environment; TRP, transient receptor potential; VP, vanilloid phytochemical

I. INTRODUCTION

A. Vanilloid Phytochemicals

A variety of plants from both the monocot and eudicot clades produce compounds that contain the 4-hydroxy-3-methoxybenzyl group (Figure 1A). This family of compounds can be collectively referred to as the "vanilloid phytochemicals," (VPs) and many members of this family have medicinal value [1,2]. The family derives its name from vanillin (Figure 1A), a compound from the pods of certain orchids that gives flavor to foods like ice cream. Vanillin has a healing effect on some brain diseases, including Parkinson's disease, Alzheimer's disease, Huntington's disease, and depression [3]. Vanillin also has an antinociceptive effect, as demonstrated in mice with acetic acid-induced pain [4]. Unlike vanillin, some VPs are well known for being pungent [5]. One such compound is capsaicin (Figure 1B), which causes the burning sensation from chili peppers. Capsaicin combats postherpetic neuralgia and other forms of neuropathic pain [6]. Research in rats suggests that one way capsaicin exerts its antinociceptive effect is by activating glutamatergic neurons in the periaqueductal gray matter [7]. Another pungent VP is 6-gingerol (Figure 1C), which causes the slight burning sensation from ginger rhizomes [5,8]. 6-Gingerol has anti-cancer properties [8] and reduces both acetic acid-induced and formalin-induced pain [9]. Two other VPs are important to introduce because we have studied them in our lab previously [10], and the present study is a continuation of those studies. One is incarvillateine (Figure 1D), which comes from the asterid *Incarvillea sinensis* and can inhibit formalin-induced pain [11,12]. The other is ferulic acid (Figure 1E), which is named for the giant fennel (*Ferula communis*) [13] but

can be found in the cell walls of a wide variety of plants, including grasses, sugar beets, and spinach [13,14]. Ferulic acid has several medicinal effects, including rescue of insulin levels in diabetes, protection of liver cells from toxicity, protection of skin cells from carcinogenesis due to ultraviolet light [15], and inhibition of neuropathic pain [16]. In summary, VPs have medicinal effects on multiple organ systems, and there is a strong connection between VPs and pain relief. In this study, we explored the potential of VPs as pain therapeutics.

B. Pain

Several cellular signaling pathways are involved in the transmission of pain. For example, three members of the transient receptor potential (TRP) family play a prominent role in mediating pain sensation at the peripheral level where the noxious stimulus is first detected [17]. TRPA1 is important for the detection of painful mechanical stimuli [18] and pain-inducing chemicals like formalin and hydrogen peroxide [19]. TRPV1 plays a major role in mediating the pain response to heat [19], and TRPM8 is involved in the pain response to cold [17]. Another relevant protein family is the voltage-gated sodium channels (VGSCs), which are necessary for action potential generation in all human neurons. Although the involvement of VGSCs as a family is unsurprising, what is more noteworthy is that some VGSCs play more of a role in pain transduction than others. For example, VGSC subtype Na_v 1.8 is especially abundant at free nerve endings and is especially important for repetitive neuronal firing. Both of these traits make Na_v 1.8 important for pain transduction, as demonstrated in Na_v 1.8 knockout mice. Such mice did not respond to painful stimuli as much as wild-type mice, and this was true regardless

of whether the painful stimulus was thermal, mechanical, or chemical [20]. Some mediators of inflammatory pain include the cyclooxygenase (COX) enzymes, which in the context of tissue damage are responsible for converting arachidonic acid into prostanoid molecules like prostaglandin E_2, which can bind to prostanoid receptors and generate pain signals. The well-known anti-inflammatory drugs aspirin, ibuprofen, and acetaminophen all work by inhibiting COX enzymes [21]. In the central nervous system, glutamate receptors, such as *N*-Methyl-D-aspartate (NMDA) receptors and α-amino-3-hydroxy-5-methyl-4-isoxazolepropionic acid (AMPA) receptors, are involved in the transmission of pain signals [22]. NMDA receptors in the spinal cord that have the NR2B subunit are especially critical in relaying pain signals [23]. Finally, experiments with knock-out mice have demonstrated that δ, κ, and μ opioid receptors are all involved in the body's ability to inhibit pain signals [24]. Opioid receptors, which are part of the large family of G-protein-coupled receptors (GPCRs) [24], perform this inhibitory action at both the peripheral and central levels [25]. The complex nature of pain signaling helps to explain why, despite decades of research on the formulation of analgesic medications, chronic pain remains one of the most serious clinical problems facing the biomedical community.

According to the International Association for the Study of Pain, chronic pain is defined as "pain without apparent biological value that has persisted beyond the normal tissue healing time," which is normally interpreted to be three months [26–28], although sometimes six months is used [28]. The most common sites for chronic pain include the back, legs, neck, shoulders [29], knee, hip [30], orofacial region, and head ("head" in this

case means the phenomenon of "headache," which is separate from orofacial pain) [31]. Chronic pain affects roughly 30% of the global population, over 2.3 billion people [26]. The prevalence of chronic pain varies substantially by country, with estimates varying from 8.7% (Singapore) to 60.4% (Ukraine). Contrary to what one might predict, chronic pain prevalence does not correlate with human development index [29]. An example of a country on the lower end of the prevalence spectrum is the United States, where daily chronic pain is estimated to affect 11.2% of adults or 25.3 million people [27]. A survey of fifteen European countries plus Israel found a moderately low prevalence of chronic pain, 19% of adults [28]. Other countries with a moderately low prevalence include India, Canada, and South Africa, with chronic pain rates of 18.3% to 19.3% of adults [26,30,32]. In contrast, Brazil has a moderately high prevalence at 39% [33].

From the mid-1990s until recently, the principal pharmacologic treatment for chronic pain was administration of opioids, such as hydrocodone, propoxyphene, codeine, oxycodone, morphine, tramadol, and fentanyl [34,35]. However, between 1999 and 2007, the number of deaths related to opioid drugs rose throughout the world and more than tripled in the USA [36]. In response, studies have been initiated to discover new analgesics with a lower risk of addiction. Among the non-opioid receptor families, the adenosine receptors have shown promise as a target for analgesics [37–42].

C. Adenosine Receptors

Adenosine is a nucleoside that has several functions, chief of which is the preservation of metabolic homeostasis. Nervous, cardiovascular, immune, respiratory, urinary, and gastrointestinal systems all benefit from the protection afforded by adenosine

receptor (AR) signaling [43]. The International Union of Pharmacology has described four receptors for adenosine (A_1, A_{2A}, A_{2B}, and A_3), all of which are GPCRs. Like other GPCRs, each AR is an integral membrane protein (IMP) whose salient structural feature is seven α helices that span the membrane. The type of G protein to which an AR is coupled varies by subtype. A_1AR and A_3AR are coupled to inhibitory G proteins (G_i), which depress cAMP levels, while A_{2A}AR and A_{2B}AR are coupled to stimulatory G proteins (G_s), which elevate cAMP levels [44]. The four receptor subtypes differ substantially from each other both in their distribution and in their physiological effects [43] and are therefore usually studied separately [45]. To date, only one of the subtypes has a selective ligand that is approved for clinical use, namely A_{2A}AR, whose agonist regadenoson (Lexiscan) is used in perfusion imaging of the heart. The only other AR ligand approved for clinical use is a non-selective agonist, namely adenosine itself (Adenocard, Adenoscan), which is used for treatment of supraventricular tachyarrythmia [46]. Although there are currently only two AR ligands approved for clinical use, the ARs have been the subject of more than three hundred studies [as reviewed by Borea et al. in 43]. All four AR subtypes have been investigated for their potential as targets for analgesic drugs [6-9].

A_1ARs are widely distributed within the human brain, with especially high concentrations in the hippocampus, striatum, and cortex [47]. They are also found in the human heart [48,49], kidney [50], and pancreas [51]. A_1ARs are distributed throughout the neural pathways that transmit pain signals, from sensory nerve endings to the dorsal horn of the spinal cord to supraspinal sites [52]. Of the four AR subtypes, A_1AR is the

most important for the antinociceptive action of endogenous adenosine [53]. Moreover, A_1ARs are part of the signaling pathway that mediates the antinociceptive effect of morphine [54]. Accordingly, A_1AR has received substantial attention as a potential drug target. Binding of agonistic molecules to A_1AR is associated with pain relief [55,56], implying that A_1AR is antinociceptive. The principal barrier to the development of A_1AR-targeted analgesics is the concern over side effects [42]. Adenosine itself is prescribed as a heart-slowing drug, and A_1AR is the subtype that mediates this action [57]. In patients with an overactive heart, slowing heart rate is beneficial, but this action represents a dangerous side effect in patients with normal heart rates. Even though this cardiovascular action may be mitigated through the use of allosteric modulators of A_1AR [53], there is still risk.

A_{2A}ARs are found primarily outside the CNS [40], especially on leukocytes and in the cells of blood vessel walls [43]. Moreover, the majority of A_{2A}ARs that are involved in pain pathways are those outside the CNS [58]. A_{2A}AR knockout mice show a reduced ability to feel pain, implying that peripheral A_{2A}ARs are pro-nociceptive [58]. This hypothesis was confirmed through the testing of a synthetic A_{2A}AR antagonist, which was analgesic [39]. The role of A_{2A}ARs in the CNS is less clear. For example, sleep deprivation is associated with higher pain sensitivity, and this effect is thought to be partially mediated by A_{2A}ARs within the nucleus accumbens [59]. However, another study of injections of A_{2A}AR ligands into the spinal cord found that an A_{2A}AR agonist relieved pain, implying that A_{2A}ARs in the spinal cord are antinociceptive [60]. Since A_{2A}ARs are also found in blood vessel walls, the possibility of cardiovascular side effects

must be considered [42]. In fact, A_{2A}AR agonists lower blood pressure [61], and it can be inferred that A_{2A}AR antagonists administered as pain medications might raise blood pressure, a concerning side effect.

A_{2B}ARs are widely distributed outside the CNS, including cells of the intestines, lungs, and immune system [43]. The distribution of A_{2B}ARs in the CNS is limited [40], although they are present on glial cells [43]. In mice tested for their pain response to a hot plate, five A_{2B}AR antagonists all showed an analgesic effect [62]. Thus, A_{2B}ARs are pro-nociceptive, like their peripheral A_{2A}AR counterparts. Not only are A_{2B}ARs pro-nociceptive, evidence suggests that A_{2B}AR plays a greater role than any of the other four receptor subtypes in the perception of pain related to systemically elevated adenosine. Antagonists of all four subtypes were tested on mice, but only the A_{2B}AR antagonist reduced the hyperalgesia [63]. An important limitation of A_{2B}ARs is that most of their effect on pain is exerted through immune cells [63]. As a result, A_{2B}ARs represent an excellent therapeutic target for inflammatory pain. However, their utility in the treatment of other chronic pain conditions is limited.

In situ hybridization studies in rats have found that A_3ARs are widely distributed in the brain, particularly in the striatum, olfactory bulb, nucleus accumbens, hippocampus, hypothalamus, thalamus, and cerebellum. Outside the CNS, A_3ARs are found at especially high densities in the spleen, lung, uterus, and testis [64]. The administration of A_3AR agonists has been shown to correlate with reduced pain [42,65–67]. Thus, A_3ARs are antinociceptive, like their A_1AR counterparts. Some evidence suggests that pain relief from A_3AR activation results from modification of the release of

the inhibitory neurotransmitter γ-aminobutyric acid (GABA) [68]. Other evidence suggests that the mechanism is A_3AR modulation of serotonergic and adrenergic neurons at the interface between the spinal cord and the medulla oblongata [42]. In any case, one of the most useful traits of A_3AR agonists is that they block the pain induced by chemotherapy drugs without hindering the anti-cancer effect [38]. A_3AR agonists accomplish this, in part, by improving the health of spinal glial cells by inhibiting NADPH oxidase [69]. Also useful is the fact that A_3AR agonists relieve pain without the concerning cardiovascular side effects observed with A_1AR and A_{2A}AR ligands [68,70]. A_3AR agonists have been tested in clinical trials for rheumatoid arthritis [71], hepatocellular carcinoma [72], and psoriasis [73] and have in all cases been demonstrated to be safe. Finally, experiments with mice in withdrawal from morphine show that A_3AR agonists can lessen withdrawal symptoms, indicating that even if A_3AR cannot replace opioids, they may be a good adjunct therapy to opioids [54]. Because of their wide distribution, strong evidence of antinociceptive activity, and lack of negative side effects, A_3AR is the most promising candidate as a target for analgesics out of the four subtypes [70].

D. Interaction of Vanilloid Phytochemicals with Adenosine Receptors

Thus far, we have established the two main foundations of the current project, namely that there is 1) a strong connection between VPs and the treatment of pain and 2) a strong connection between ARs and the treatment of pain. Based on these two facts, we hypothesized that ARs might play a role in mediating the antinociceptive action of VPs. Data consistent with this hypothesis are found in previous studies, which have

demonstrated that the antinociceptive action of the VP incarvillateine is probably mediated by ARs [10,12]. Accordingly, we initially attempted to study incarvillateine in this project, but we had difficulties purifying it. We then decided to study curcumin (CUR), a VP that bears a structural resemblance to incarvillateine in that it also has two vanillyl moieties (Figures 1 and 2).

E. Curcumin and *cis-trans* Curcumin

CUR comes from the herb *Curcuma longa*, which grows in Asia. Clinical trials have repeatedly demonstrated that CUR is an effective anti-cancer and anti-inflammatory agent [74–76], and clinical data also support the efficacy of CUR in the treatment of neurodegenerative diseases, liver disease, cardiovascular disease, diabetes, psoriasis, alcohol intoxication, and other diseases [74–76]. The principal barrier to the use of CUR as a medication is its low bioavailability. CUR is poorly absorbed by the digestive system, and what little is absorbed is rapidly metabolized to give products, such as ferulic acid. These facts limit the biodistribution of CUR and limit its serum concentration in particular, thus drastically reducing its effectiveness [77]. This limitation has been partially overcome through a variety of techniques in recent years. Some researchers complexed curcumin with cyclodextrin and thereby achieved reductions in the size of lung tumors [78]. Others created micelles that are enriched with curcumin, which can be absorbed via the microfold cells of the intestine [79]. The most attractive answer to the CUR bioavailability problem, however, has been nanoparticles. Over four hundred studies have investigated the efficacy of nanoformulations of CUR [as reviewed by Yallapu et al. in 80], and one such study successfully used CUR nanoparticles to reduce

levels of inflammatory cytokines and reduce fibrosis in a mouse model of liver disease [81]. In short, solutions to the poor bioavailability of CUR that has hindered its translation into clinical use are being actively pursued.

CUR is effective in the treatment of autoimmune inflammation [82] and postoperative pain [83]. Previous work has demonstrated that CUR exerts its antinociceptive effects in part by acting as a COX pathway inhibitor [84] and a TRPV1 antagonist [85]. Based on evidence that ARs are responsible for the antinociceptive action of incarvillateine, we hypothesized that they might have a role in the antinociceptive action of CUR as well, alongside COX and TRPV1. However, some of our preliminary assays indicated that CUR may not bind well to ARs. We then became interested in the AR interactions of a synthetic vanilloid compound we had created as part of a separate study. The compound was created by using cavitand-mediated photoisomerization to change one of the two non-aromatic, carbon-carbon double bonds in CUR (highlighted in Figure 2) from trans to cis, while leaving the other one trans. The IUPAC name of the compound is (1*E*,6*Z*)-1,7-bis(4-hydroxy-3-methoxyphenyl)hepta-1,6-diene-3,5-dione. We gave the compound a common name, "*cis-trans* curcumin" (CTCUR) (shown in Figure 3). Our preliminary studies indicated that CTCUR bound to ARs, and we decided to elucidate the binding and receptor activation of CTCUR further.

F. Statement of Hypothesis

In summary, our study fills important gaps in the scientific literature in two ways. First, we are discovering information about the pharmacological action of CTCUR, a novel stereoisomer of CUR. Second, we are discovering generalizable information about

the interaction of VPs with ARs. This knowledge could aid in the treatment of chronic pain. Accordingly, our central hypothesis has been that CTCUR may alleviate pain by activating A_1AR or A_3AR, or by inhibiting A_{2A}AR or A_{2B}AR.

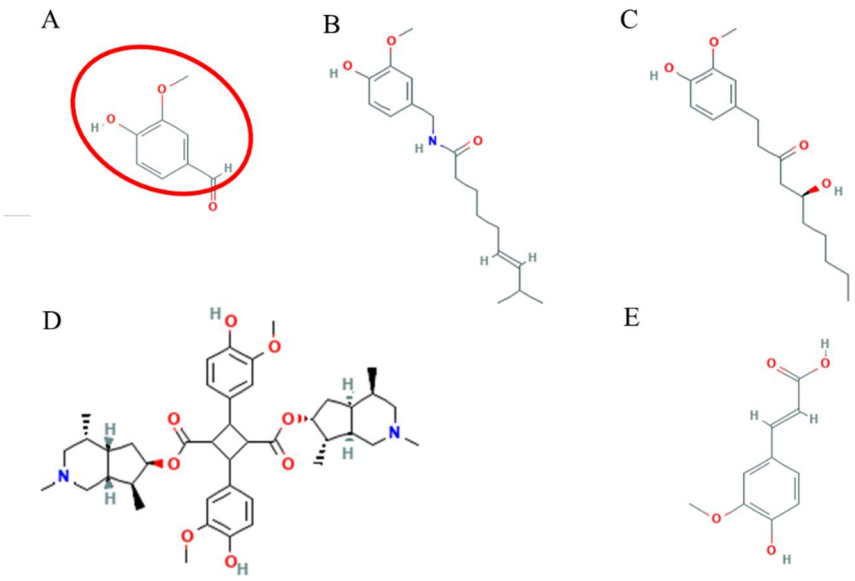

Figure 1. Chemical structures of A) vanillin (PubChem CID 1183) with the 4-hydroxy-3-methoxybenzyl group—also called a vanillyl group— circled in red, B) capsaicin (PubChem CID 1548943), C) 6-gingerol (PubChem CID 3473), D) incarvillateine (PubChem CID 9875096), and E) ferulic acid (PubChem CID 445858).

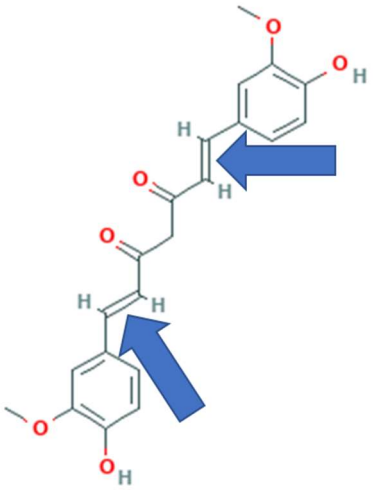

Figure 2. Chemical structure of curcumin (PubChem CID 969516) with the two non-aromatic, carbon-carbon double bonds highlighted with blue arrows. The isomerization process used in this study altered one of these double bonds, leaving the other unchanged.

II. MATERIALS AND METHODS

A. Chemical Synthesis

CTCUR synthesis was achieved through photochemical cavitand-mediated isomerization. Relative to structurally similar cinnamic acids, CUR is resistant to photoisomerization. This resistance is most likely due to excited state proton transfers that occur when the molecule is in its enol form. This obstacle was overcome through the cavitand-mediation approach. CUR (50 mg) was added to water (20 mL) containing one equivalent of γ-cyclodextrin. The mixture was stirred with heating at 70 °C for 1 h. The cooled solution was further stirred for 3 h during which a chalky slurry of the inclusion complex resulted. The resulting mixture was irradiated for 48 h in a photochemical irradiation chamber (Ace Glass Inc., Vineland, NJ, USA; product no. 7836-20) with a medium pressure mercury vapor lamp (Ace Glass Inc., Vineland, NJ, USA; 450 W; 121.92 mm arc length; product no. 7825-34). The irradiated mixture was de-complexed by adding water (50 mL) to the slurry and stirring with ethyl acetate (50 mL). The organic layer was isolated and dried over anhydrous magnesium sulfate, then the solvent was removed under vacuum. The mixture was subjected to gravity chromatography on a silica gel column with 0.1% formic acid in dichloromethane. The yellow-colored CTCUR was isolated in 8% yield. The presence of CTCUR was confirmed by proton nuclear magnetic resonance (^{1}H NMR) and gas chromatography–mass spectrometry (GCMS).

The gas chromatography column was Agilent HP-5 (5%-phenyl)-methylpolysilane nonpolar. The initial temperature was 100 °C; the initial time was 1 min; the heating rate was 10.0 °C/min; the final temperature was 300 °C; and the final

time was 5 min. Retention time of CTCUR was 6.8 min. ^{1}H NMR ($CDCl_3$, 400 MHz) data were as follows: 8.08 ppm (m, 1H); 7.98 ppm (d, 1H); 7.66 ppm (d, 1H); 7.40 ppm (t, 1H); 7.11 (m, 2H); 7.05 (s, 1H); 6.94 ppm (d, 1H); 6.48 ppm (d, 1H); 6.32 ppm (d, 1H); 3.98 (s, 3H); 3.93 (s, 3H). Mass spectrometry data were as follows, in the format m/z (relative %, ion): **367** (5, M^+), **351** (3, M^+ - OH), **245** (5, M^+ - Ar-OMe), **191** (100, M^+ - CH=CH-CO), **177** (90, M^+ - CH_2), **149** (30, - CO), **123** (10, M^+ - CH=CH).

B. Cell Culture

For the G_s-linked receptors, two human embryonic kidney-293 (HEK-293) cell lines transfected with human A_{2A}AR and human A_{2B}AR, respectively, were purchased from Perkin Elmer (Waltham, MA, USA). Cells were cultured in Eagle's minimum essential medium (EMEM) supplemented with 10% fetal bovine serum (FBS). For the G_i-linked receptors, two Chinese hamster ovary-K1 (CHO-K1) cell lines transfected with human A_1AR and human A_3AR, respectively, were purchased from Perkin Elmer (Waltham, MA, USA). Cells were cultured in Ham's F12 medium supplemented with 10% FBS. For all four cell lines, the first two passages after thawing were cultured without antibiotic to allow recovery from thawing stress, then all subsequent passages were cultured with 400 μg/mL geneticin (Thermo Fisher Scientific, Waltham, MA, USA) to select for transfected cells.

C. Competitive Binding Assays

Cells were seeded at 30,000 cells per well onto a black-walled 96-well plate with transparent well bottoms and were allowed to incubate for approximately two days. Once

confluence was achieved, wells were treated with either A) media only, B) media + test compound at 10^{-5} M, C) media + fluorescent compound at 60 nM, or D) media + fluorescent compound at 60 nM + test compound at varying concentrations. The test compound was either CUR or CTCUR, and the fluorescent compound was CA200623 CellAura fluorescent adenosine agonist, a derivative of 5'-N-Ethylcarboxamidoadenosine (NECA) (HelloBio, Princeton, NJ, USA). After a 2 h incubation, cells were washed twice with 1X phosphate-buffered saline (PBS). Dulbecco's modified Eagle's medium (DMEM) with no phenol red indicator was then added (100 µL per well) to prevent desiccation during reading. The plate was read with a Synergy H1 microplate reader (BioTek, Winooski, VT, USA) in top read mode. To generate a binding curve from competitive binding assay (CBA) data, a percent fluorescence change was calculated for each treatment (eq. 1-3). These values were in turn used to calculate the inhibitory constant (K_i) (see section H, Statistical Analysis, below).

$$\text{Control fluorescence} = (\text{fluorescence of CA200623}) - (\text{fluorescence of media})$$

Equation 1.

$$\text{Treatment fluorescence} = (\text{fluorescence of CTCUR} + \text{CA200623}) - (\text{fluorescence of CTCUR})$$

Equation 2.

$$\%\ \text{fluorescence change} = \frac{\text{Treatment fluorescence}}{\text{Control fluorescence}} * 100\%$$

Equation 3.

During this project, attempts were made to optimize the protocol described above. It was discovered that white-walled plates with opaque well bottoms produce superior

results compared to black-walled plates with transparent well bottoms. Furthermore, it was discovered that washing once with 1X PBS produces superior results compared to washing twice. Thus, it is recommended that future studies employ white-walled plates and wash once.

D. Docking Studies

Preparation of protein structures

The X-ray crystal structures of A_1AR (Protein Data Bank ID: 5UEN) [86] and A_{2A}AR (Protein Data Bank ID: 5NM4) [87] were retrieved from the RCSB Protein Data Bank. Both proteins were prepared in the Molecular Operating Environment (MOE) [88], and the side chain and ligand atoms were optimized, first with the main chain atoms fixed in order to reduce steric repulsion and at the same time to minimize the perturbation to the main chain structure. After that, the whole structure was optimized using Assisted Model Building with Energy Refinement (AMBER) force field. There were no crystal structures of A_{2B}AR and A_3AR. Thus, homology models for A_{2B}AR and A_3AR were built using the Homology Model module in MOE, using human A_{2B}AR sequence (GenBank: AAA51598.1) and human A_3AR sequence (GenBank: CAA54288.1) as query sequences, respectively. The template structure to build the homology models was A_{2A}AR crystal structure 5NM4. After the homology model were built, structural alignment to the template 5NM4 was carried out in MOE to evaluate the quality of the model proteins. The model proteins were optimized first with main chain atom fixed and then further optimized with all atoms being relaxed. The homology models of A_{2B}AR and A_3AR were

aligned to 5NM4, and the ligand in 5NM4 was adopted to the homology model proteins to help identify the binding pocket for docking studies.

The MOE optimized proteins (A_1AR, A_{2A}AR, A_{2B}AR, and A_3AR) were imported to Maestro 12.4 and were subsequently prepared using the Protein Preparation Wizard in the Schrödinger software suite 2020.2 [89]. In the Protein Preparation Wizard, the side-chain structures of glutamine and asparagine were allowed to flip to maximize H-bond interactions. Proteins were subjected to 500 iterations of energy minimization with backbone atoms being restrained using the Optimized Potentials for Liquid Simulations (OPLS) force field in the MacroModel module in the Schrödinger software [89].

Preparation of ligand structures

To study the binding selectivity between AR subtypes, compounds A, B, and KW3902 (NAX) were built as controls, along with CTCUR in its EZ-keto form (Figure 3). All ligands were built in MOE [88] and were optimized using a Merck Molecular Force Field 94 (MMFF94) using default settings. The optimized ligands were then exported to Maestro for docking studies. All imported ligands in Maestro were further minimized using the OPLS force field in the MacroModel module in the Schrödinger software [89].

Glide docking procedures

Grid files for each of the four proteins were generated using the Glide Grid Generation protocol with the bound ligands as centroids. Ligands were docked to each of the grid files, which defined the binding pockets of respective proteins. During the docking process, the scaling factor for receptor van der Waals for the nonpolar atoms was

set to 0.8 to allow for some flexibility of the receptor, and an extra-precision method was used to calculate the docking scores. All other parameters were set to default. The binding affinity was expressed in terms of change in free energy (ΔG). The more negative the ΔG, the more favorable the interaction of the complex. In order to compare ΔG values derived from docking with K_i values derived from CBAs, K_i values were converted to ΔG values (eq. 4).

$$\Delta G = RT \ln Ki \left(\frac{kcal}{mol}\right)$$

Equation 4.

E. Confocal Fluorescence Microscopy

Cells were seeded onto 12-well glass-bottom plates (Cellvis, Mountain View, CA, USA). For the HEK-293 lines, cells were seeded at 700,000 cells per well. For the CHO lines, seeding density was reduced to 375,000 cells per well because that is consistent with the seeding density we used for CBAs. Seeding at 375,000 cells per well in a 12-well plate is roughly equivalent to seeding at 30,000 cells per well in a 96-well plate. In either case, the cells were incubated for two days to reach confluence. On the day images were collected, cells were treated with either A) media only, B) CTCUR at 1 μM, C) CA200623 at 60 nM, or D) CA200623 at 60 nM + CTCUR at 1 μM. Our microscopy protocol was a modification of a previously published one [90]. Cells were incubated for 1.5-2.0 h, washed with 1X PBS, immersed in DMEM with no phenol red indicator, and viewed with a 60× oil immersion objective and an Olympus FV3000 laser scanning confocal microscope (Olympus, Tokyo, Japan). For the HEK-293 cell lines, we washed

twice with 1X PBS. For the CHO-K1 cell lines, we washed once with 1X PBS, because our attempts to optimize CBAs had demonstrated that washing once yields superior results compared to washing twice. For the HEK-293 lines, images were acquired at a resolution of 512 by 512 pixels. For the CHO-K1 lines, images were acquired at a resolution of 640 by 640 pixels, because it was decided that the slightly longer acquisition time was justified in order to obtain better images (compared to 512 by 512 pixels). For the media-only and CTCUR-only treatments, a single location within the well was imaged. For the CA200623-only and the CA200623/CTCUR combination treatments, three representative locations within the well were imaged. At each location, a stack of images at 0.5 μm intervals in the z-axis were acquired. All images were processed using CellSens Dimension Desktop V1.18 (Olympus). A constrained iterative deconvolution was performed on each stack of images. To reduce bias in selecting individual images out of the stacks, we employed the following method. First, each stack of images was reviewed to see how many images were usable for analysis. The uppermost usable image was called the "upper boundary," and its number within the stack was noted. That number was divided by the total number of images within the stack to yield the "upper boundary as fraction." The same was done with the lowermost usable image in the stack to yield the "lower boundary as fraction." After this process was completed on all stacks, the results were averaged to yield the "average upper boundary as fraction" and the "average lower boundary as fraction." We expected the best image to be the one halfway between the upper boundary and the lower boundary. Thus, we averaged the "average upper boundary as fraction" and the "average lower boundary as

fraction" to yield the "average best image as fraction." The "average best image as fraction" was 62% for our A_{2B} cells, 65% for our A_{2A} cells, 64% for our A_1 cells, and 61% for our A_3 cells. Finally, for each stack we selected one image for analysis by multiplying the "average best images as fraction" by the total number of images in that stack.

Quantitative analysis was done with ImageJ [91] using a modification of a protocol from the Queensland Brain Institute [92]. The freehand selection tool in ImageJ was used. The background fluorescence level was determined by measuring the mean gray value (MGV) of the media-only image. For each selected image from the CA200623 only and the CA200623/CTCUR combination treatments, nine cells were selected to be analyzed. One was the cell at the middle of the image, four were the cells midway between the middle of the image and each of the four corners of the image, and four were the cells midway between the middle of the image and the four midpoints of the four edges of the image. The corrected mean gray value (CMGV) for each cell was calculated according to equations 5 and 6.

$$\text{CTCF} = (\text{Integrated density}) - (\text{Area of selected cell}) * (\text{MGV of background fluorescence})$$

Equation 5. CTCF is corrected total cell fluorescence. MGV is mean gray value.

$$\text{CMGV} = \frac{\text{CTCF}}{\text{Area of selected cell}}$$

Equation 6. CMGV is corrected mean gray value. CTCF is corrected total cell fluorescence.

F. Cytotoxicity Assays

Cytotoxicity assays were performed using previously described methods [93]. In brief, cells were seeded at 8,000 cells per well in 96-well plates, and after overnight incubation, they were treated with different concentrations of CUR or CTCUR for 2 h (the same time point used for binding assays). The compounds were dissolved in DMSO at a concentration of 0.1 M and diluted for assays as required. Cell survival was measured using PrestoBlue dye (Thermo Fisher Scientific, Waltham, MA, USA) per manufacturer's instructions, and fluorescence was measured at 560 nm/ 590 nm (excitation/emission) using a Synergy H1 microplate reader and Gen5 software (BioTek, Winooski, VT, USA). Percent change was calculated relative to the average for control cells (no treatment).

G. Cyclic Adenosine Monophosphate Immunoassays

Cells were seeded at 50,000 cells per well in a 96-well plate and allowed to incubate overnight. After running our first twenty cyclic AMP assays, we reduced this seeding density down to 35,000 cells per well to ensure that the cells would still be in log phase when they were treated the next day (i.e., to ensure that the cells would not reach confluence overnight). After the overnight incubation, cells were treated with test compounds or control solutions and allowed to incubate for 2 h.

To test for antagonism in the G_s-linked cell lines, 600 nM NECA was used as a control agonist, and CTCUR was added to see if it would decrease the agonistic activity of NECA. To test for agonism in the G_i-linked cell lines, 50 μM forskolin was used as a

control stimulator of adenylate cyclase, and CTCUR was added to see if it would activate the G_i-linked receptors and mitigate the effect of forskolin. Note that the forskolin was added at the 1 h 45 min mark, such that cells were only incubated with the forskolin for 15 min. After incubation was complete, the lysing of the cells and the remaining parts of the assay were performed according to the manufacturer's protocol (ab138880 cAMP Direct Immunoassay Kit, Abcam, Cambridge, UK). The plate was read with a Synergy H1 microplate reader (BioTek, Winooski, VT, USA).

Attempts were made to test for agonism in the G_s-linked cell lines by adding CTCUR alone, without NECA. However, these tests for agonism were run before our cyclic AMP assay procedure was optimized. Specifically, samples for these tests were diluted 1:10 before analysis, unlike later tests, in which we did not dilute the samples. Because the baseline concentration of cyclic AMP in the cells being studied was ~5-15 nM, diluting 1:10 reduced the concentration to ~0.5-1.5 nM, which is at the limit of detection for the kit being used (see above). Data from these tests for agonism are therefore inaccurate and were excluded from later analyses. We did not test for antagonism in the G_i-linked cell lines due to the difficulty of those experiments, which were beyond the scope of this project.

H. Statistical Analysis

For each CBA dataset, the inhibitory constant was calculated according to the Cheng-Prusoff equation [94] (eq. 7). For fluorescence microscopy, the CMGVs from the CA200623-only and the CA200623/CTCUR combination treatments were compared with

unpaired t-tests. If the assumptions of the t-test were violated, a Mann-Whitney test was used. For cyclic AMP assays, treatments were compared via ordinary one-way ANOVA with Tukey's multiple comparisons test. If the assumptions of the ANOVA were violated, a Kruskal-Wallis test with Dunn's multiple comparisons test was used. K_i calculations, tests to compare treatments, and tests to assess the normality and homoscedasticity of datasets, were all performed with Prism 8.4.3 (GraphPad, San Diego, CA, USA). For all analyses, $p < 0.05$ was considered significant ($\alpha = 0.05$).

$$K_i = \frac{IC_{50}}{1 + \frac{[L]}{K_d}}$$

Equation 7. K_i is the inhibitory constant. IC_{50} is the test compound concentration when half of binding is inhibited. [L] is the concentration of the fluorescent compound. K_d is the dissociation constant of the fluorescent ligand, equal to $\frac{[\text{fluorescent ligand}]^x[\text{receptor}]^y}{[\text{ligand}-\text{recep} \quad \text{complex}]}$.

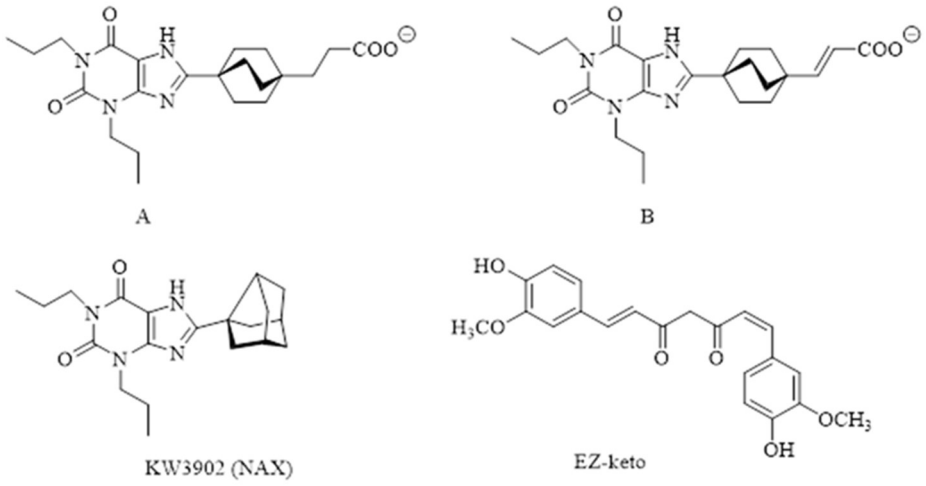

Figure 3. Structures of compounds A, B, and KW3902 (NAX), which were used as controls, and CTCUR in its EZ-keto form.

III. RESULTS

A. Adenosine Receptor Subtype A_1

CUR showed a reduction in cell survival for A_1AR-transfected CHO cells at 100 μM (37% survival compared to control, Figure 4C). Data from 100 μM treatments of CUR was therefore excluded from binding analysis. The K_i from the resulting dataset was 1.55 X 10^{-7} M (Figure 4A). CUR also showed moderate toxicity at 10 μM (58% survival compared to control), and we therefore excluded the 10 μM CUR data as well. However, doing so resulted in a K_i of 2.22 X 10^{-8} M, the lowest K_i value observed in this study. Given the weak affinity of CUR for the other three AR subtypes (Figures 8A, 12A, 16A), this low value is probably inaccurate. It was therefore concluded that measuring a K_i for CUR at A_1AR is not possible using our methodology. Measuring a K_i in this case would require introducing a correction factor into the K_i calculation to account for cell death.

CTCUR showed no reduction in cell survival from 1 nM through 100 μM (Figure 4D). Binding assays indicate that the K_i of CTCUR at A_1AR is 3.06 X 10^{-7} M (Figure 4B). Confocal microscopy results corroborate this finding. A Mann-Whitney U test of the CMGVs of cells viewed through the microscope indicated that CTCUR at 1 μM significantly blocked the binding of CA200623 to A_1AR-transfected CHO cells ($p < 0.0001$, Figure 5). Docking studies indicate that CTCUR binds to A_1AR at the extracellular end of transmembrane helix 3, the extracellular linking region between helices 4 and 5, and the extracellular end of helix 6 [86] (Figure 6). Docking indicated a

ΔG for CTCUR at A_1AR of -10.217 kcal/mol, which implies 13% stronger binding compared to our experimental ΔG value, which was -8.89 kcal/mol. The experimental ΔG value was derived from the K_i value reported above. Immunoassay results also support the hypothesis that CTCUR binds to A_1AR. Forskolin + 10 μM CTCUR produced a 27.5 nM reduction in cAMP concentration compared to the forskolin control (Figure 7). Since A_1AR is G_i-linked, the observed reduction in cAMP concentration in response to CTCUR suggests that CTCUR acts as an agonist at A_1AR.

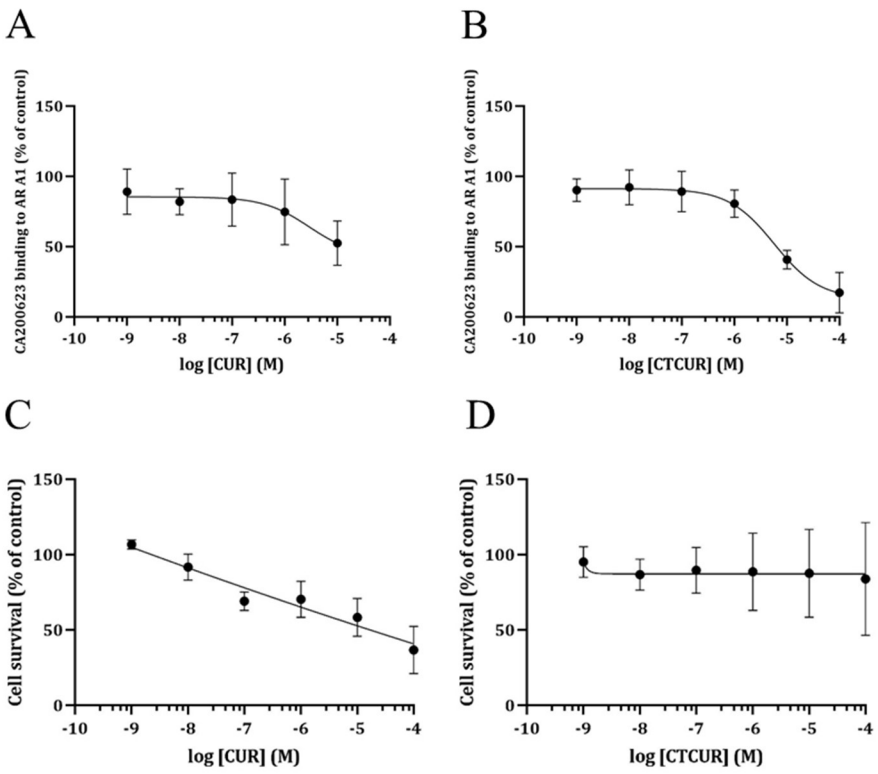

Figure 4. (A) Binding curve showing competition of CUR with a fluorescent AR ligand (CA200623) at A_1AR (n = 3, K_i not measurable). (B) Binding curve showing competition of CTCUR with a fluorescent AR ligand (CA200623) at A_1AR (n = 3, K_i = 306 nM). (C) Survival curve for A_1AR-transfected CHO cells treated with CUR (n=3). Survival was reduced to 58% at 10 μM and to 37% at 100 μM. (D) Survival curve for A_1AR-transfected CHO cells treated with CTCUR (n = 5). There was no reduction in cell survival. (A-D) Bars indicate standard deviation.

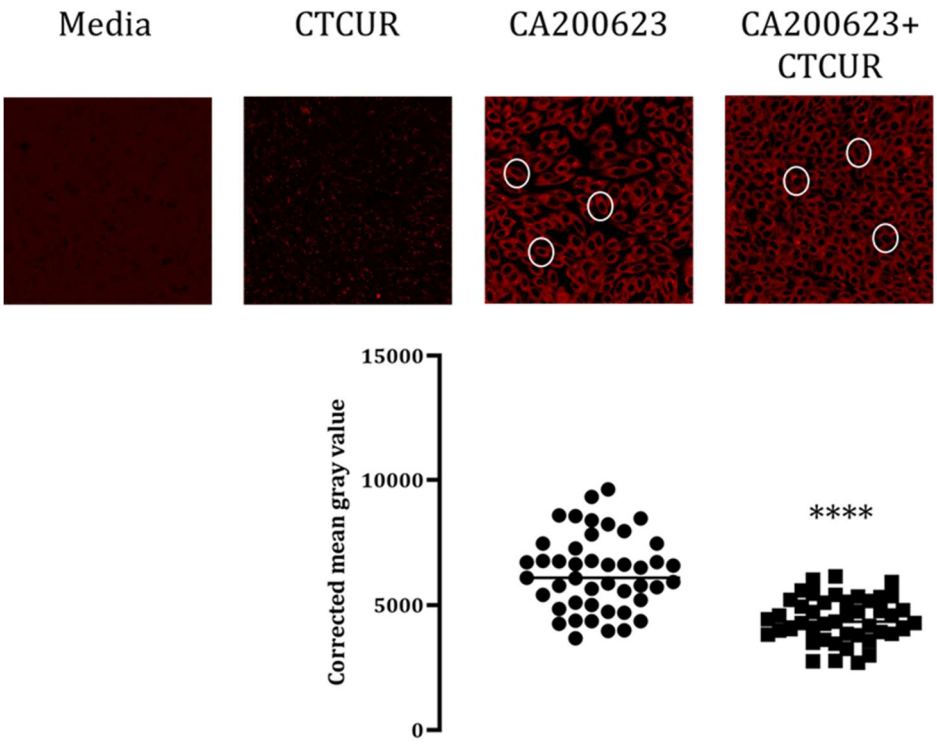

Figure 5. Competitive binding assay of CTCUR and a fluorescent AR ligand (CA200623) at A_1AR viewed through a confocal microscope. White circles highlight individual cells. For the CA200623 treatment, two wells were selected, three image stacks were collected from each well, and nine cells were selected from each image stack. The same was done for the CA200623 + CTCUR treatment. Each dot within the corrected mean gray value scatterplot represents one cell. Each cluster of dots corresponds to the treatment indicated above it (**** indicates $p < 0.0001$).

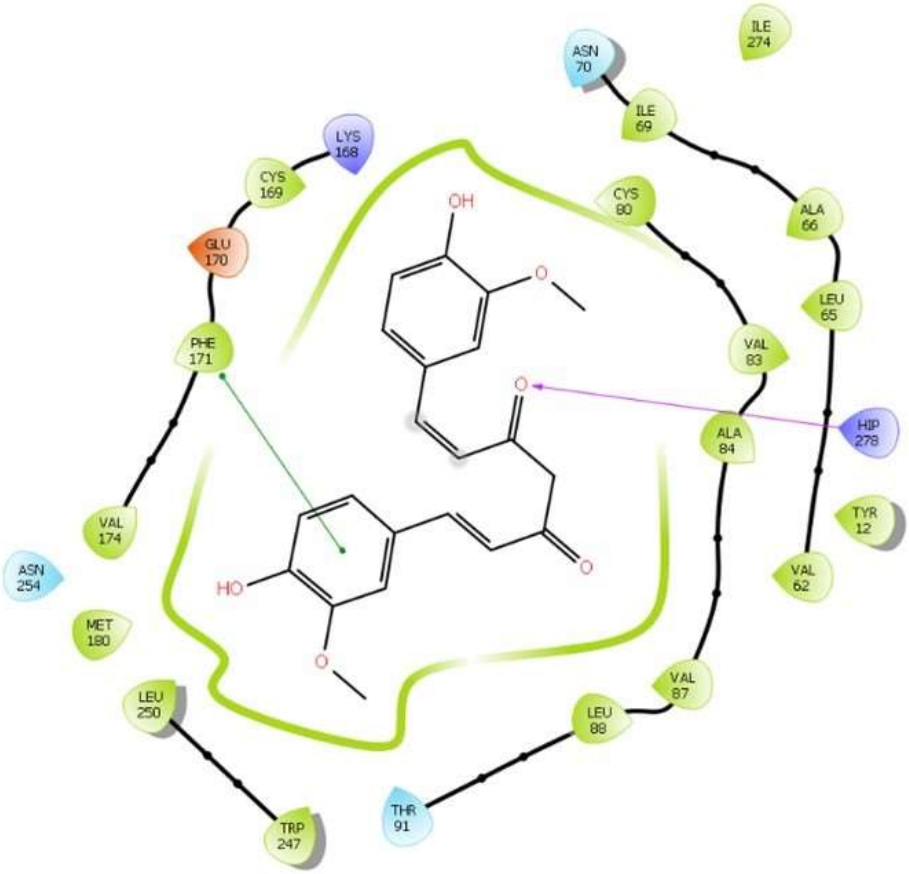

Figure 6. Computer model of the interaction between CTCUR and amino acids of A_1AR. ΔG = -10.217 kcal/mol.

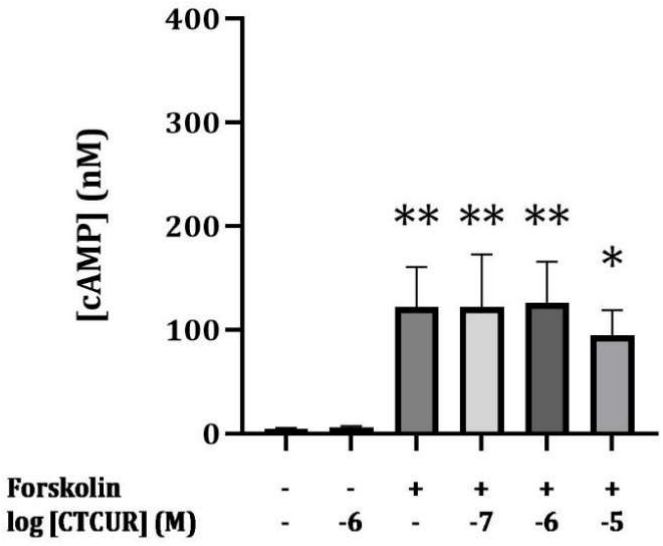

Figure 7. Test for agonistic activity of CTCUR at A_1AR (B, n = 3). Forskolin was administered at 50 μM to directly activate adenylate cyclase and thereby elevate cAMP levels. Since A_1AR is G_i-linked, reduction in cAMP levels indicates agonism of the receptor. Asterisks indicate significant difference from both the media control (-, -) and the CTCUR control (-, -6). * indicates $0.01 < p \leq 0.05$, ** indicates $p \leq 0.01$. Bars indicate standard deviation.

B. Adenosine Receptor Subtype A_3

CUR showed moderate reduction in cell survival at 100 μM (65% survival compared to control, Figure 8C), and 100 μM results were therefore excluded from binding analysis. CUR did not show any appreciable binding to A_3AR (K_i > 10,000,000 nM, Figure 8A). CTCUR showed no reduction in cell survival from 1 nM through 100 μM (Figure 8D). Binding assays indicate that the K_i of CTCUR at A_3AR is 4.00 X 10^{-7} M (Figure 8B). Confocal microscopy results did not confirm this finding. The average CMGV of cells treated with 60 nM CA200623+1 μM CTCUR was 11,315, which is higher than the average CMGV for cells treated with 60 nM CA200623 alone, namely 8,846 (Figure 9). This elevation in CMGV implies that CTCUR fluoresced at 657 nm, the same wavelength at which CA200623 fluoresces. However, our competitive binding assay results have consistently shown that cells treated with 10 μM CTCUR do not fluoresce at 657 nm any more than cells treated with media. We therefore conclude that these microscopy results for A_3AR are inaccurate. Examination of the morphology of the cells provided a potential explanation for this error. The cells in the CA200623-only wells displayed the expected CHO cell morphology. Each cell was roughly an oval, and the membranes of the respective cells tended to be separated from each other. The cells in the CA200623+CTCUR wells, however, were abnormal. The membranes of the respective cells were meshed together, giving the overall image a web-like appearance, much like the pattern that is typically seen with HEK-293 cells (Figures 9, 13, and 17). Although this difference in morphology explains the discrepancy in the CMGV results, the difference in morphology itself is more difficult to explain. The cells were plated at

the same time and at the same density, and therefore should have displayed a consistent morphology. Docking studies indicated that CTCUR binds to A_3AR at the extracellular end of transmembrane helix 3, the center and extracellular end of helix 6, the extracellular linking region between helices 6 and 7, and the extracellular end of helix 7 [95] (Figure 10). Docking indicated a ΔG for CTCUR at A_3AR of -10.934 kcal/mol, which implies 20% stronger binding compared to our experimental ΔG value, which was -8.73 kcal/mol (derived from the K_i we obtained from our binding assays). A Kruskal-Wallis test of the receptor activation data found a significant difference between the groups in general ($p = 0.032$), but the follow-up Dunn's test did not find any significant differences between particular pairs of groups (Figure 11). There was a 23.84 nM reduction in cAMP concentration in response to the forskolin + 10 μM CTCUR treatment compared to the forskolin control. Although not statistically significant, this result is consistent with the receptor activation results for A_1AR, and it thus supports the hypothesis that CTCUR acts as an agonist of ARs.

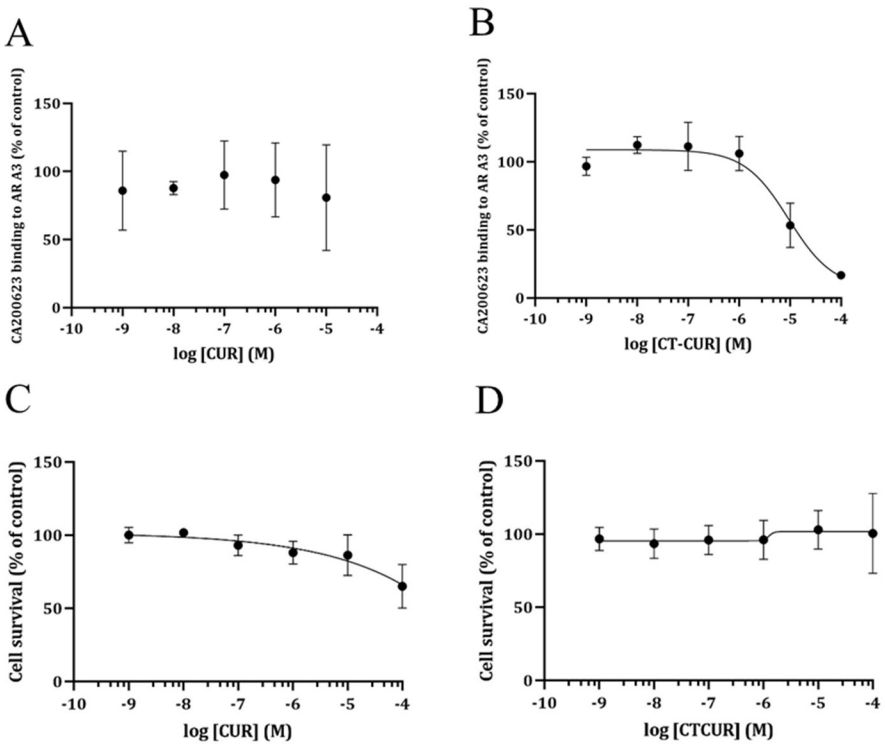

Figure 8. (A) Binding data showing competition of CUR with a fluorescent AR ligand (CA200623) at A_3AR. No curve is shown because the data are statistically equivalent to a flat line (n = 3, K_i > 10,000,000 nM). (B) Binding curve showing competition of CTCUR with a fluorescent AR ligand (CA200623) at A_3AR (n = 3, K_i = 400 nM). (C) Survival curve for A_3AR-transfected CHO cells treated with CUR (n = 3). Survival was reduced to 65% at 100 μM. (D) Survival curve for A_3AR-transfected CHO cells treated with CTCUR (n = 6). There was no reduction in cell survival. (A-D) Bars indicate standard deviation.

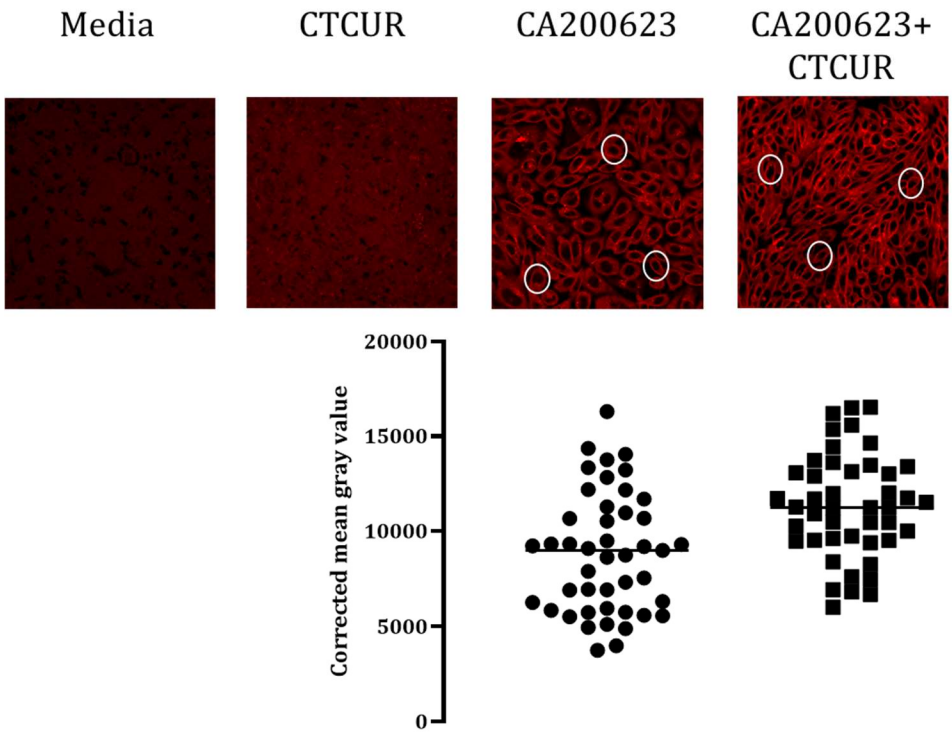

Figure 9. Competitive binding assay of CTCUR at A_3AR viewed through a confocal microscope. White circles highlight individual cells. For the CA200623 treatment, two wells were selected, three image stacks were collected from each well, and nine cells were selected from each image stack. The same was done for the CA200623 + CTCUR treatment. Each dot within the corrected mean gray value scatterplot represents one cell. Each cluster of dots corresponds to the treatment indicated above it.

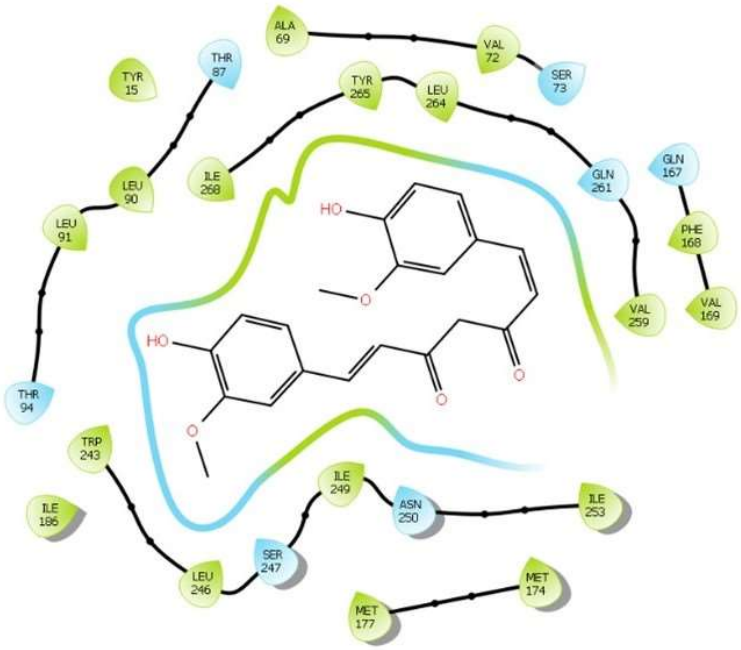

Figure 10. Computer model of the interaction between CTCUR and amino acids of A_3AR. ΔG = -10.934 kcal/mol.

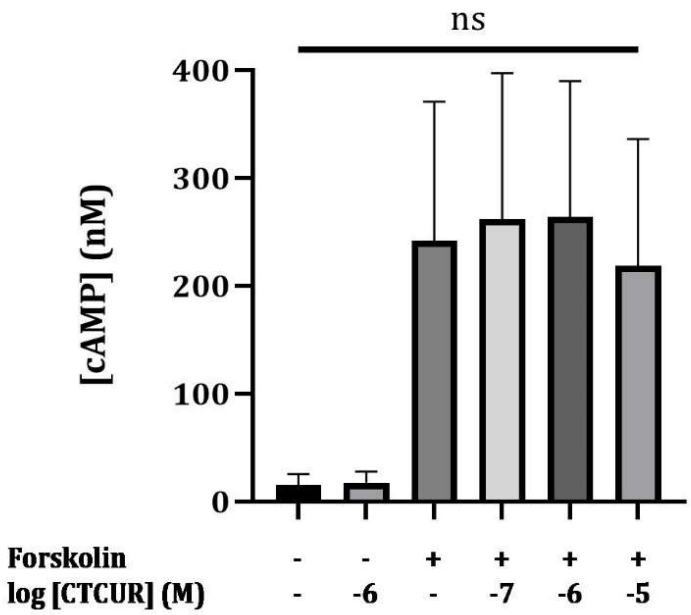

Figure 11. Test for agonistic activity of CTCUR at A_3AR (B, n = 3). Forskolin was administered at 50 μM to directly activate adenylate cyclase and thereby elevate cAMP levels. Since A_3AR is G_i-linked, reduction in cAMP levels indicates agonism of the receptor. Bars indicate standard deviation.

C. Adenosine Receptor Subtype A_{2A}

In competition assays, the fluorescence values from 100 μM treatments of CUR tended to be abnormally high. These values were therefore excluded. CUR showed no appreciable binding to $A_{2A}AR$ (K_i > 10,000,000 nM, Figure 12A). CTCUR at 100 μM showed a moderate reduction in cell survival in $A_{2A}AR$-transfected HEK-293 cells (68% survival compared to control, Figure 12C). However, we chose to include the data for 100 μM CTCUR at $A_{2A}AR$ to maintain consistency with our analysis of the other three subtypes, since 100 μM CTCUR did not reduce cell survival in any of the other three cell lines. The K_i for CTCUR at $A_{2A}AR$ when the 100 μM data are included is 5.11 X 10^{-6} M (Figure 12B). If the 100 μM data are excluded, then the calculated K_i is about ten times higher, namely 6.18 X 10^{-5} M. Quantitative analysis of the images from confocal microscopy indicated that the average CMGV of the cells treated with only CA200623 was 4,155, while the average CMGV of cells treated with both CA200623 and 1 μM CTCUR was 3,647. A Mann-Whitney U test indicated that this difference is not significant ($p > 0.99$), but the direction of the difference is consistent with the idea that CTCUR was able to outcompete CA200623 and bind to $A_{2A}AR$ (Figure 13). Docking studies indicated that CTCUR binds to $A_{2A}AR$ at the cytoplasmic ends of transmembrane helices 5, 6, and 7 [87] (Figure 14). Docking indicated a ΔG for CTCUR at $A_{2A}AR$ of -9.6 kcal/mol, which implied 25% stronger binding compared to our experimental ΔG value, which was -7.2 kcal/mol (derived from the K_i we obtained from our binding assays). An ANOVA of the receptor activation results indicated no significant differences among treatments ($p = 0.63$, Figure 15). Interestingly, though, the trend in the results is

the opposite of the one we had expected to find. We were testing to see whether CTCUR could act as an antagonist, blocking the activity of NECA and thus decreasing cAMP production. However, the trend suggests the opposite. The NECA + 10 μM CTCUR treatment induced a 2.0 nM increase in cAMP concentration relative to the NECA control. Since $A_{2A}AR$ is G_s-linked, this trend suggests that CTCUR may act as an agonist of $A_{2A}AR$.

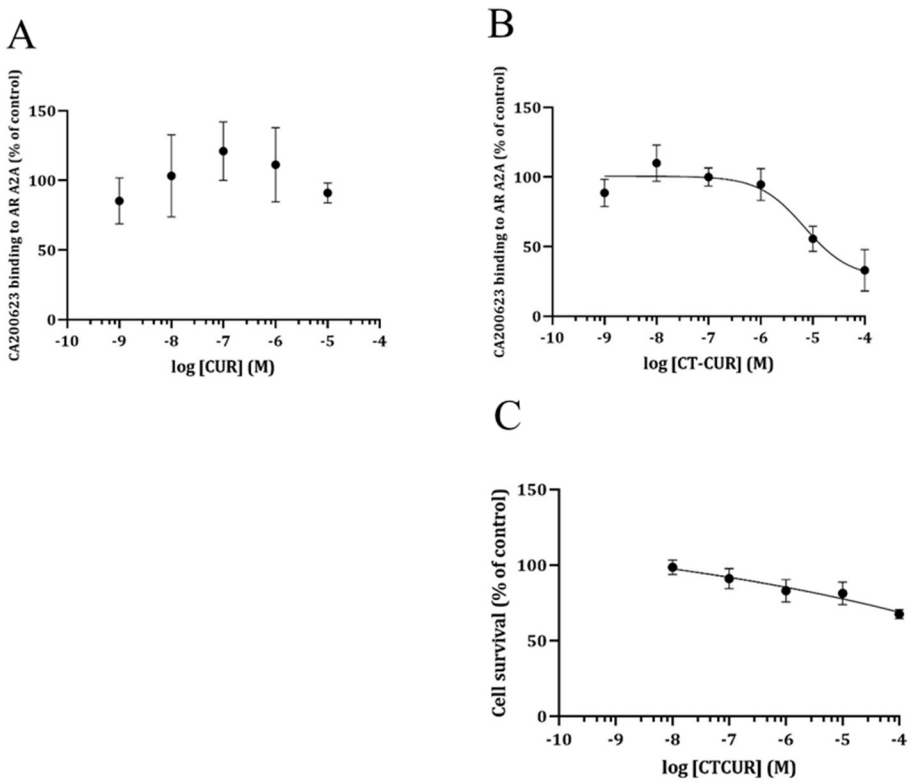

Figure 12. (A) Binding data showing competition of CUR with a fluorescent AR ligand (CA200623) at $A_{2A}AR$. No curve is shown because the data are statistically equivalent to a flat line (n = 3, K_i > 10,000,000 nM). (B) Binding data showing competition of CTCUR with a fluorescent AR ligand (CA200623) at $A_{2A}AR$ (n = 3, K_i = 5,110 nM). (C) Survival curve for $A_{2A}AR$-transfected HEK-293 cells treated with CTCUR (n = 4). Survival was reduced to 68% at 100 μM. (A-C) Bars indicate standard deviation.

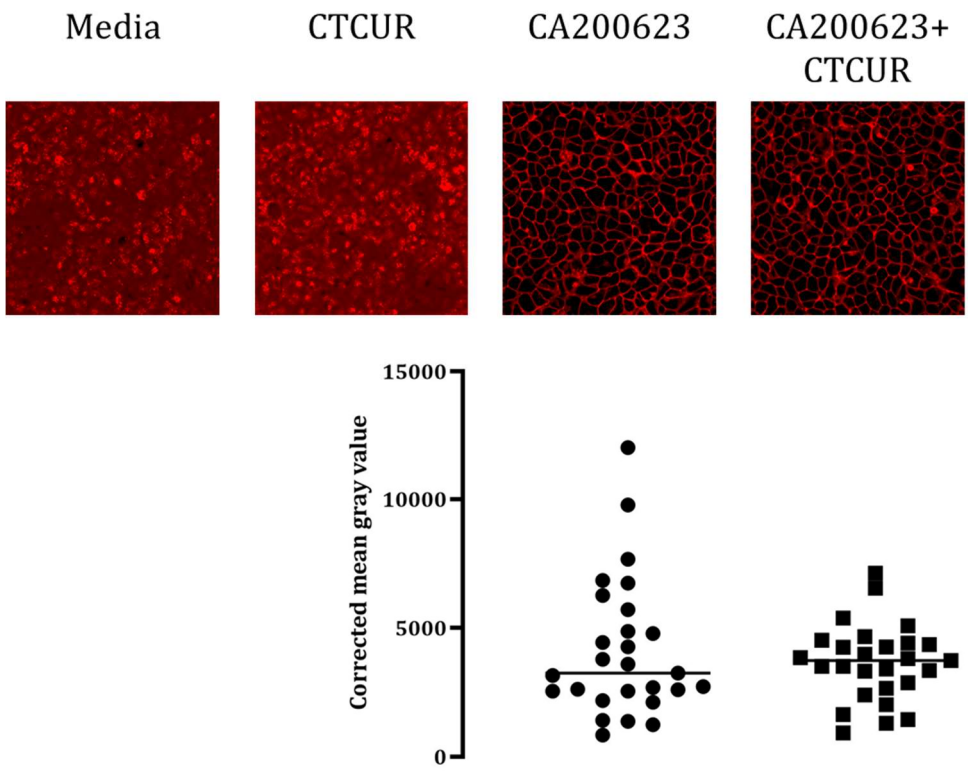

Figure 13. Competitive binding assay of CTCUR at $A_{2A}AR$ viewed through a confocal microscope. White circles highlight individual cells. For the CA200623 treatment, two wells were selected, two image stacks were collected from each well, and nine cells were selected from each image stack. The same was done for the CA200623 + CTCUR treatment. Each dot within the corrected mean gray value scatterplot represents one cell. Each cluster of dots corresponds to the treatment indicated above it.

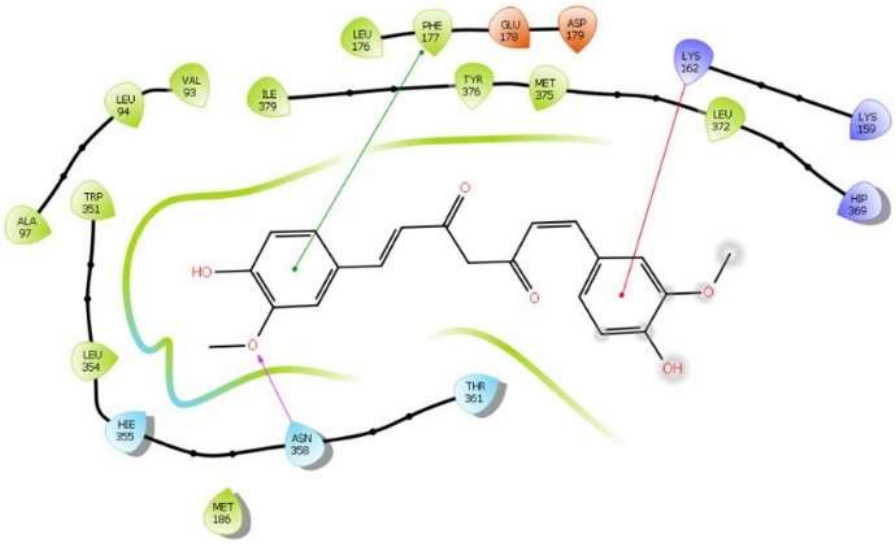

Figure 14. Computer model of the interaction between CTCUR and amino acids of $A_{2A}AR$. ΔG = -9.6 kcal/mol.

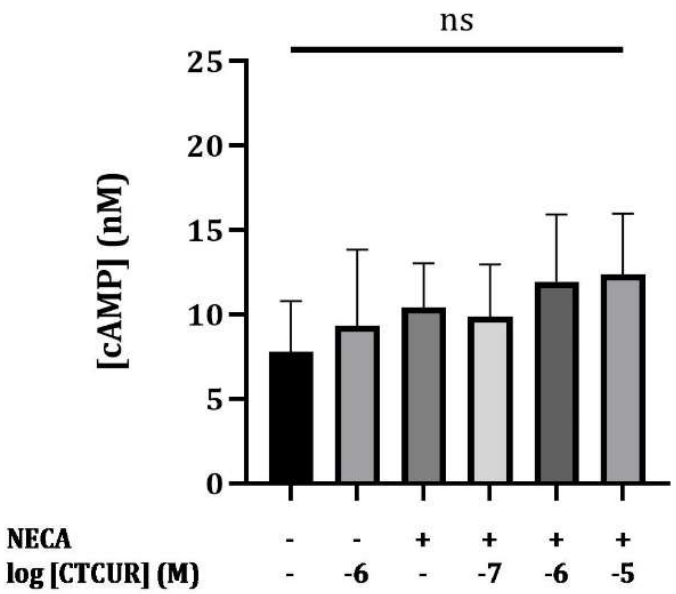

Figure 15. Test for antagonistic activity of CTCUR at $A_{2A}AR$ (B, n = 3). NECA is an AR agonist. Since $A_{2A}AR$ is G_s-linked, NECA binding elevates cAMP levels. Reduction in cAMP levels indicates competition with NECA. Bars indicate standard deviation.

D. Adenosine Receptor Subtype A_{2B}

In competition assays, the fluorescence values from 100 μM treatments of CUR tended to be abnormally high. These values were therefore excluded. CUR showed weak binding to A_{2B}AR, with a K_i of 5.70 X 10^{-3} M (Figure 16A). CTCUR showed no reduction in cell survival from 10 nM through 100 μM (Figure 16C). Binding assays indicate that the K_i of CTCUR at A_{2B}AR is 6.72 X 10^{-6} M (Figure 16B). Confocal microscopy results corroborate this finding. A two-tailed, unpaired t-test of the CMGV values of cells viewed through the microscope indicated that CTCUR at 1 μM significantly blocked the binding of CA200623 to A_{2B}AR-transfected HEK cells ($p = 0.040$, Figure 17). Docking studies indicated that CTCUR binds to A_{2B}AR at transmembrane helices 6 and 7 and at the cytoplasmic linking region near transmembrane helix 5 [96] (Figure 18). Docking indicated a ΔG for CTCUR at A_{2B}AR of -7.3 kcal/mol, which differs by only 3% from our experimental ΔG value of -7.1 kcal/mol (derived from the K_i we obtained from our binding assays). This close agreement between the ΔG values obtained from both *in vitro* and *in silico* constitutes strong evidence that CTCUR binds to A_{2B}AR with a K_i in the micromolar range. Kruskal-Wallis and Dunn's tests of the receptor activation data showed that the only significant differences between groups were those between the NECA+ 10 μM CTCUR treatment and the media control ($p = 0.015$) and between the NECA+ 10 μM CTCUR treatment and the CTCUR control ($p = 0.010$) (Figure 19). The NECA + 10 μM CTCUR treatment induced a 3.3 nM increase in cAMP concentration relative to the NECA control. Since A_{2B}AR is G_s-linked, the

increase in cAMP production in response to CTCUR implies that CTCUR acts as an agonist of A_{2B}AR.

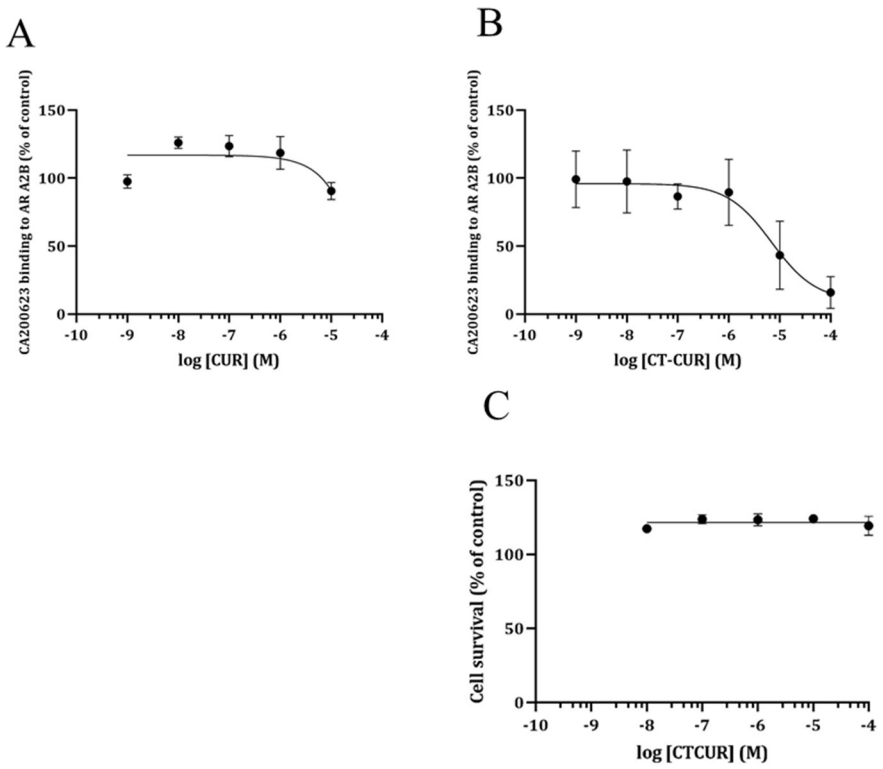

Figure 16. (A) Binding curve showing competition of CUR with a fluorescent AR ligand (CA200623) at $A_{2B}AR$ (n = 2, K_i = 5,700,000 nM). (B) Binding curve showing competition of CTCUR with a fluorescent AR ligand (CA200623) at $A_{2B}AR$ (n = 3, K_i = 6,720 nM). (C) Survival curve for $A_{2B}AR$-transfected HEK cells treated with CTCUR (n = 3). There was no reduction in cell survival. (A-C) Bars indicate standard deviation.

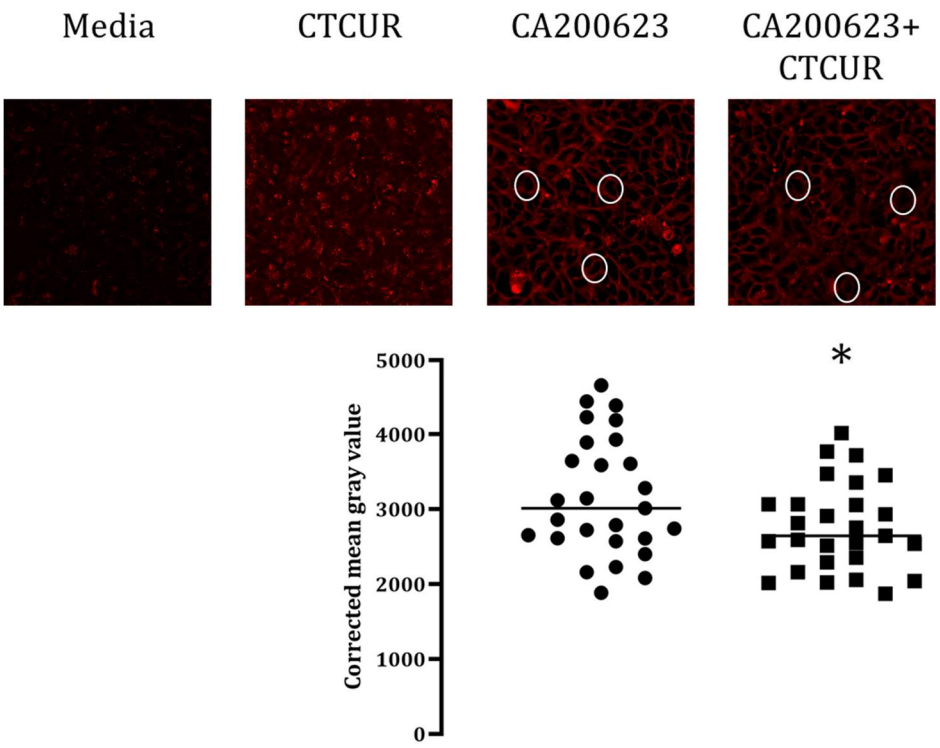

Figure 17. Competitive binding assay of CTCUR at $A_{2B}AR$ viewed through a confocal microscope. White circles highlight individual cells. For the CA200623 treatment, two wells were selected, two image stacks were collected from each well, and nine cells were selected from each image stack. The same was done for the CA200623 + CTCUR treatment. Each dot within the corrected mean gray value scatterplot represents one cell. Each cluster of dots corresponds to the treatment indicated above it (* indicates $p = 0.040$).

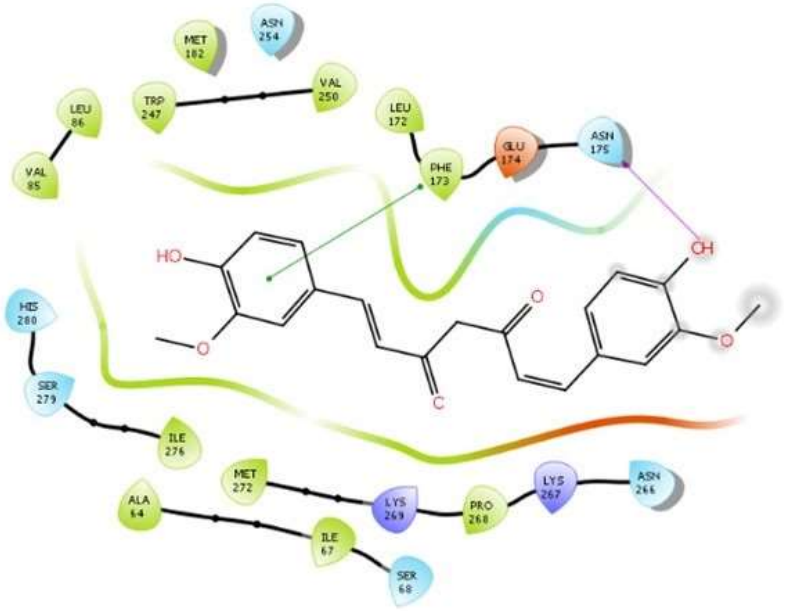

Figure 18. Computer model of the interaction between CTCUR and amino acids of $A_{2B}AR$. ΔG = -7.3 kcal/mol.

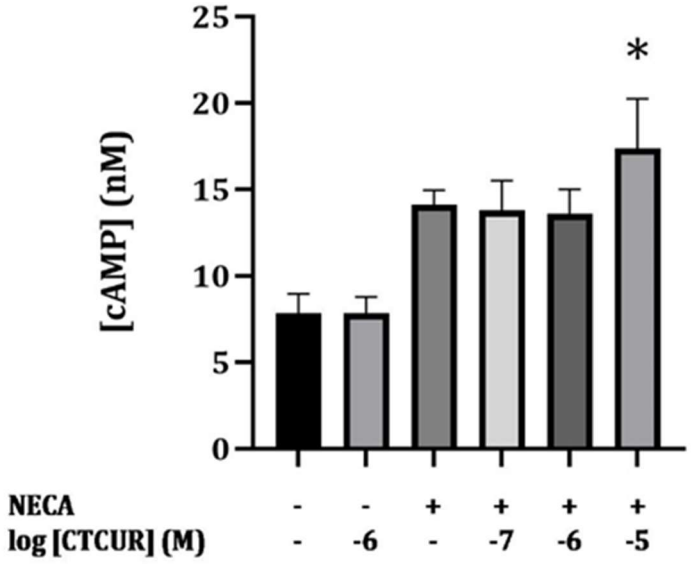

Figure 19. Test for antagonistic activity of CTCUR at $A_{2B}AR$ (B, n = 2). NECA is an AR agonist. Since $A_{2B}AR$ is G_s-linked, NECA binding elevates cAMP levels. Reduction in cAMP levels indicates competition with NECA. * indicates significant ($p < 0.05$) difference from both the media control (-, -) and the CTCUR control (-, -6). Bars indicate standard deviation.

E. Summary Tables

Table 1. Binding affinities of CUR and CTCUR in the context of other important AR ligands. Values are K_i (nM) at the human versions of each AR subtypes.

Compound*	A_1	A_3	A_{2A}	A_{2B}
CTCUR	306	400	5,107	6,722
CUR	-	>10,000,000	>10,000,000	5,700,000
Adenosine	100[a]	290[a]	310[a]	15,000[a]
NECA	14[b]	6.2[b]	20[b]	2,400[b]
Regadenoson	>16,460[c]	-	1,269[c]	>100,000[c]
Tecadenoson	2[d]	227[d]	6,390[d]	25,800[d]
Caffeine	44,900[e]	13,300[e]	23,400[e]	10,400[e]
Theophylline	6,920[f]	22,300[f]	6,700[f]	9,070[f]

a [97], b [98], c [99], d [100] e [62], f [101]

*Adenosine is an endogenous agonist and prescription drug. NECA is an agonist used in AR research. Regadenoson is an agonist used for heart imaging. Tecadenoson is an A_1AR- selective agonist that has been investigated as a drug for supraventricular tachycardia[102]. Caffeine is an antagonist whose pro-wakefulness effects are due to interaction with A_{2A}AR [103] . Theophylline is an antagonist used in AR research.

Table 2. Summary of results from the four methods used to measure the interaction of CTCUR with the four AR subtypes. This information was used to assess the selectivity of CTCUR among the subtypes.

Method	A_1	A_3	A_{2A}	A_{2B}
K_i (nM)	306	400	5,107	6,722
Visual binding (microscopy)	Confirms binding	No difference	No difference	Confirms binding
$\Delta G_{docking}$ (kcal/mol)	-10.217	-10.934	-9.6	-7.3
Cellular signaling (cAMP)	Suggests agonism	No difference	No difference	Suggests agonism

IV. DISCUSSION

The principal discovery of this study is that CTCUR, a vanilloid compound, binds to all four AR subtypes, with inhibitory constants ranging from 300 nM to 7 μM. Based on our survey of the extant AR literature, this study constitutes the first time that the binding affinity of a vanilloid compound for any AR subtype has been quantified. CTCUR binding is supported by both *in vitro* assays (Figures 4B, 8B, 12B, 16B) and *in silico* docking studies (Figures 6, 10, 14, 18). In the cases of A_1AR and A_{2B}AR, CTCUR binding is also strongly supported by microscopy data (Figures 5 and 17). The second main conclusion of this study is that CTCUR acts as an agonist of ARs, which is indicated by changes in intracellular levels of cAMP, a downstream signaling molecule to AR binding (Figures 7, 11, 15, 19). Agonist activity was observed in all four subtypes, although the evidence is stronger for A_1AR and A_{2B}AR compared to A_3AR and A_{2A}AR.

The binding affinities of CTCUR are compared to those of some established AR ligands in Table 1. For example, the affinity of CTCUR for A_1AR is similar to that of adenosine itself, the difference being approximately three-fold. The similarity of affinity for A_3AR between CTCUR and adenosine is even closer, the difference being less than two-fold. When compared to the K_i values at A_{2A}AR for regadenoson (A_{2A}AR agonist) and the caffeine (A_{2A}AR antagonist), CTCUR has a K_i at A_{2A}AR that falls within the range of the other two. Finally, CTCUR has a K_i at A_{2B}AR that is stronger than that of any of the other compounds shown, except for NECA (Table 1). Thus, it is reasonable to hypothesize that CTCUR might have a biologically relevant effect, since its affinity for ARs is comparable to that of biologically active compounds.

With respect to CTCUR's activity for the four receptor subtypes, three important observations can be made: (1) Both K_i data and ΔG data support CTCUR being selective for the two G_i-linked subtypes (A_1AR and A_3AR) over the two G_s-linked subtypes (A_{2A}AR and A_{2B}AR) (Table 2). The selectivity ratio for G_s-linked/G_i-linked is approximately 17. (2) K_i, microscopy, and receptor activation data all support CTCUR being selective for A_1AR over A_3AR (Table 2). The ΔG data, which showed stronger binding to A_3AR, were the exception. However, the difference between the ΔG values for A_1AR and A_3AR was only 7%, which means that this exception is not enough to overrule the trend from the other three methods. (3) In contrast, the data for the two G_s-linked subtypes are ambiguous. The K_i and ΔG data suggest stronger interaction with A_{2A}AR, while the microscopy and cAMP data suggest stronger interaction with A_{2B}AR (Table 2). In summary, our data suggest that of the four AR subtypes, CTCUR has the greatest affinity for A_1AR. However, the A_1AR selectivity ratios for CTCUR are small (1.3, 16.7, and 22.0 for A_3/A_1, A_{2A}/A_1, and A_{2B}/A_1, respectively) compared to the ratios for other A_1AR-selective compounds. For example, the A_3/A_1 selectivity ratio for tecadenoson is 114 (Table 1).

Having established that CTCUR binds to ARs, the next relevant question is whether CTCUR binds to the orthosteric site or to an allosteric site. A study involving the mutation of individual residues of A_{2B}AR found that W247, V250, and S279 were especially important for the biding of nucleoside agonists [96]. Our docking data show that the vanillyl moiety of CTCUR binds to all three of these key residues and thus shows a binding pattern similar to that of adenosine itself (Figure 18). The data for A_1AR

corroborate this conclusion. The orthosteric site of A_1AR was discovered in 2018 and was defined in terms of the eleven amino acids that are within 4 Å of adenosine when it is bound. The eleven residues are V87, T91, F171, E172, M180, W247, L250, N254, I274, T277, H278 [104]. CTCUR is predicted to interact with ten of these eleven (Figure 6), indicating that when CTCUR binds A_1AR, it occupies the orthosteric site.

ARs are part of the rhodopsin-like family of GPCRs [105], and as such it is thought that the W residue within the C/S W X P domain of transmembrane helix 6 (that is, W247) is important for A_1AR activation [86,105,106], though some data contradict this hypothesis [96]. Docking predicts that the vanillyl moiety of CTCUR interacts with this same C/S W X P domain in all four receptor subtypes (W247 in Figure 6, W243 in Figure 10, W351 in Figure 14, W247 in Figure 18), thus one would expect that CTCUR acts as an agonist of ARs. Our cAMP immunoassay data from all four subtypes were consistent with this expectation. Relative to the positive control for each assay, treatment with 10 μM CTCUR induced a 23% decrease in cAMP levels for A_1AR (Figure 7), a 10% decrease for A_3AR (Figure 11), a 19% increase for A_{2A}AR (Figure 15), and a 23% increase for A_{2B}AR (Figure 19). These changes in cAMP concentration are comparable to those seen in a study of AR-transfected CHO cells treated with adenosine. Adenosine treatment decreased forskolin-induced cAMP production in cells transfected with A_1AR and A_3AR but increased cAMP production in cells transfected with A_{2A}AR and A_{2B}AR [107]. Compared to 10 μM CTCUR, 10 μM adenosine produced greater decreases in cAMP levels (> 50% decrease relative to forskolin control) but smaller increases in cAMP levels (< 0.1 nmol increase relative to baseline) [107].

Cytotoxicity assays indicated that CTCUR is less toxic compared to its parent compound, CUR (Figures 4C&D, 8C&D, 12C, 16C). Neither compound reduced cell survival between 1 nM and 1 μM. But at 100 μM, CUR was more toxic than CTCUR. For A_{2A}AR and A_{2B}AR cells, CUR was sufficiently toxic at 100 μM that coherent CBA results could not be obtained. For A_1AR and A_3AR cells, consistent CBA results could be obtained at 100 μM, but cytotoxicity assays showed reduction in cell survival to 51% of control (average of A_1AR and A_3AR data) (Figures 4C and 8C). In contrast, CTCUR showed no reduction in cell survival at 100 μM for three of the four cell lines (Figures 4D, 8D, 16C). Some toxicity was observed in A_{2A}AR cells treated with 100 μM CTCUR (68% of control survival) (Figure 12C), but this toxicity was not as severe as the toxicity observed for 100 μM CUR (51% of control survival). It should be noted that the primary purpose of these cytotoxicity assays was to act as a control for the CBAs, ensuring that any reduction in fluorescence observed was due to competition rather than cell death. As such, the treatment time was set to mimic that of a CBA, namely 2 h. This short treatment time means that the relevance of these results to *in vivo* toxicity must be interpreted with caution, and that preference should be given to data from clinical trials in which the effects of prolonged exposure are measured. Clinical trials in patients with knee osteoarthritis [108,109] and major depressive disorder [110] have shown that CUR is safe for humans when administered at 1 g per day. One clinical trial with cancer patients demonstrated that even 8 g of CUR per day for three months does not produce any toxic effects [111]. This is true because 8 g administered orally translates to a maximum serum concentration of 1.8 μM, well below the 100 μM at which CUR is toxic [111].

As mentioned previously, our competitive binding assay results consistently indicated that cells treated with 10 μM CTCUR did not fluoresce at 657 nm any more than cells treated with media. Based on this, our protocol for analyzing images obtained from microscopy only involved a correction for the background fluorescence coming from media and cells. There was no additional correction for background fluorescence from CTCUR. However, the microscopy images show, to varying extents, that 1 μM CTCUR fluoresced more than the media control (Figures 5, 9, 13, 17). An Olympus representative whom we contacted regarding this issue indicated that this trend was most likely observed because the detection range for the microscope was broader than the detection range for the microplate reader used for CBAs. Thus, the possibility that fluorescence from CTCUR may have affected the microscopy results must be considered. If fluorescence from CTCUR was detected from the microscope, then the reduction in fluorescence observed as a result of CTCUR binding would be smaller compared to the reduction that would have been observed if no fluorescence from CTCUR was detected. Therefore, the fact that there was a significant difference between treatment groups observed for A_1AR (Figure 5) and A_{2B}AR (Figure 17) is true even if fluorescence from CTCUR was a confounding variable. Including a correction for fluorescence from CTCUR would only have made the groups even more significantly different.

When viewing our results in the context of the extant literature on the receptor pharmacology of VPs, the most noteworthy connection is that our results are consistent with those of a study that indicated that the VP incarvillateine binds to ARs [12]. Contradicting our results, though, is another study which indicated that the vanilloid

moiety of incarvillateine was not important for its antinociceptive properties, suggesting that instead the cyclobutane and monoterpene alkaloid moieties are more important [112]. Next, it is important to note that the antinociceptive effects of VPs are sometimes mediated by TRPV1, as demonstrated in studies of CUR [85] and capsaicin [7]. It is generally accepted that the vanillyl moiety is important for the binding of these compounds to TRPV1 [113], and docking studies have confirmed that the vanillyl moiety plays a key role in the binding of capsaicin to TRPV1 [114]. A comparison of the binding of CTCUR to ARs with the binding of other VPs to TRPV1 is therefore warranted. For example, the interaction of capsaicin with TRPV1 has an EC_{50} of 712 nM [115]; the interaction of CUR with TRPV1 has an IC_{50} of 67 nM [85]; and the interaction of 6-Shogaol with TRPV1 has an EC_{50} of 200 nM [116,117]. Since there is a rough correspondence among EC_{50}, IC_{50}, and K_i values, these data mean that the inhibitory constant for the interaction of VPs with TRPV1 generally falls between 10 nM and 1 μM. In contrast, the inhibitory constant for the interaction of CTCUR with ARs (determined by this present study) is about one order of magnitude weaker, ranging from 100 nM to 10 μM (Table 2). Finally, within the literature on unmodified CUR there is one study that examined AR interactions. The study examined mouse models of epileptic seizure and found that the anti-seizure effect of unmodified CUR is mediated by A_1AR [118]. Our study found that unmodified CUR generally does not bind to ARs (Figures 4A, 8A, 12A, 16A). However, in the case of A_1AR, a K_i was not able to be calculated due to cytotoxicity. It seems plausible, therefore, to hypothesize that unmodified CUR does bind to A_1AR, but not to the other AR subtypes.

Besides the benefits of modulating ARs in the context of relieving pain, these receptors have medicinal applications across several organ systems, which have been extensively reviewed [43]. For example, A_1AR agonism in the heart can suppress atrioventricular node activity [102] and sinoatrial node activity [119], and thereby correct tachycardia. A_{2A}AR agonism is also beneficial in the heart, where A_{2A}AR activity exerts an anti-inflammatory effect. In hypertensive rats with experimentally induced myocardial infarctions, the administration of the A_{2A}AR agonist LASSBio-294 prevents fibrosis and tumor necrosis factor α secretion [120]. A_{2B}AR agonism is beneficial in the pancreas and liver, where A_{2B}AR activation helps to maintain a healthy response to insulin. In mice that were fed a high fat diet to induce metabolic dysfunction, administration of the A_{2B}AR agonist BAY 60-6583 lowered plasma glucose and plasma insulin levels, improved insulin sensitivity, and restored proper levels of insulin receptor substrate 2. This evidence suggests that A_{2B}AR agonists could be used to treat type 2 diabetes [121]. Finally, because A_3AR is overexpressed in cancer cells, A_3AR agonists are effective in combating cancer of the skin, prostate, colon, and liver [122]. A_3AR agonists can also work in the immune system to calm inflammation, as shown by the success of the A_3AR-selective agonist piclidenoson in ameliorating rheumatoid arthritis [123]. This brief survey of AR pharmacology demonstrates that an AR ligand can have vastly different effects depending on which subtype it binds to and which organ system it is present in. Improving subtype selectivity and improving localization of drug delivery are therefore important considerations in the effort to translate AR ligands into effective medications.

One limitation of the current study is that only transfected cells were used. Future work could include binding studies of CTCUR to primary glial cells isolated from animal models. Another limitation was our inability to calculate a K_i for unmodified CUR at A_1AR, and future work could address this by controlling for cell death in the K_i calculation. Future binding studies could also measure the interaction of other VPs with ARs, giving priority to compounds that have established antinociceptive behavior, such as incarvillateine and capsaicin. Another limitation was that the cAMP immunoassay data collected in this study were not sufficient to assess the strength of the agonistic activity of CTCUR relative to the agonistic activity of adenosine. Future cAMP assays could include both adenosine and CTCUR so that the two can be compared directly. It should be noted that, from the perspective of pain medicine, weak agonistic activity is sometimes better than strong agonistic activity. Previous work with partial A_1AR agonists has shown that they can effect analgesia without causing the cardiovascular side effects associated with full agonists [37,124]. Finally, the prediction from this study that CTCUR might induce analgesia could be confirmed via administration of CTCUR in a rodent model. If analgesia is observed, then CTCUR could be co-administered with an A_1AR-selective antagonist, then with an A_3AR-selective antagonist. If either antagonist prevents the analgesic effect, then the interaction of CTCUR with ARs will be confirmed *in vivo*, adding to the *in vitro* and *in silico* evidence from this study.

In summary, given that VPs are known to have a therapeutic effect on pain, and given that ARs are known to mediate pain, it is unfortunate that almost no literature exists on the interaction of VPs with ARs. Our hypothesis was that CTCUR, a VP, might

alleviate pain by activating A_1AR or A_3AR, or by inhibiting A_{2A}AR or A_{2B}AR. Since CTCUR is selective for A_1AR and A_3AR over A_{2A}AR and A_{2B}AR, and since CTCUR displays agonistic activity, we fail to reject our hypothesis.

V. LITERATURE CITED

1. Hail N. Mechanisms of vanilloid-induced apoptosis. *Apoptosis*. 2003;8(3):251-262.

2. Imm J, Zhang G, Chan L, Nitteranon V, Parkin KL. [6]-Dehydroshogaol, a minor component in ginger rhizome, exhibits quinone reductase inducing and anti-inflammatory activities that rival those of curcumin. *Food Res Int*. 2010;43:2208-2213. doi:10.1016/j.foodres.2010.07.028

3. Anand A, Khurana R, Wahal N, et al. Vanillin: a comprehensive review of pharmacological activities. *Plant Arch*. 2019;19:1000-1004.

4. Park S, Sim Y, Choi S, et al. Antinociceptive profiles and mechanisms of orally administered vanillin in the mice. *Arch Pharm Res*. 2009;32(11):1643-1649. doi:10.1007/s12272-009-2119-8

5. Prescott J, Stevenson RJ. Pungency in food perception and preference. *Food Rev Int*. 1995;11(4):665-698. doi:10.1080/87559129509541064

6. Hayman M, Kam PCA. Capsaicin: a review of its pharmacology and clinical applications. *Curr Anaesth Crit Care*. 2008;19:338-343. doi:10.1016/j.cacc.2008.07.003

7. Starowicz K, Maione S, Cristino L, et al. Tonic endovanilloid facilitation of glutamate release in brainstem descending antinociceptive pathways. *J Neurosci*. 2007;27(50):13739-13749. doi:10.1523/JNEUROSCI.3258-07.2007

8. Wang S, Zhang C, Yang G, Yang Y. Biological properties of 6-gingerol: a brief review. *Nat Prod Commun*. 2014;9(7):1027-1030. doi:10.1177/1934578X1400900736

9. Young H, Luo Y, Cheng H, Hsieh W, Liao J-C, Peng W-H. Analgesic and anti-inflammatory activities of [6]-gingerol. *J Ethnopharmacol*. 2005;96:207-210. doi:10.1016/j.jep.2004.09.009

10. Priebe A, Hunke M, Tonello R, et al. Ferulic acid dimer as a non-opioid therapeutic for acute pain. *J Pain Res*. 2018;11:1075-1085.

11. Nakamura M, Chi Y, Yan W, et al. Strong antinociceptive effect of incarvillateine, a novel monoterpene alkaloid from *Incarvillea sinensis*. *J Nat Prod*. 1999:1293-1294. doi:10.1021/np990041c

12. Wang M, Yu G, Yi S, et al. Antinociceptive effects of incarvillateine, a monoterpene alkaloid from *Incarvillea sinensis*, and possible involvement of the adenosine system. *Sci Rep*. 2015;5(16107):1-11. doi:10.1038/srep16107

13. Kim JK, Park SU. A recent overview on the biological and pharmacological activities of ferulic acid. *EXCLI J*. 2019;18:132-138. doi:doi.org/10.17179/excli2019-1138

14. Mathew S, Abraham TE. Ferulic acid: an antioxidant found naturally in plant cell walls and feruloyl esterases involved in its release and their applications. *Crit Rev Biotechnol*. 2004;24:59-83. doi:10.1080/07388550490491467

15. Gohil KJ, Kshirsagar SB, Sahane RS. Ferulic acid--a comprehensive pharmacology of an important bioflavonoid. *Int J Pharm Sci Res*. 2012;3(1):700-710.

16. Xu Y, Lin D, Yu X, et al. The antinociceptive effects of ferulic acid on neuropathic pain: involvement of descending monoaminergic system and opioid receptors. *Oncotarget*. 2016;7(15):20455-20468.

17. Julius D. TRP channels and pain. *Annu Rev Cell Dev Biol*. 2013;29:355-384. doi:10.1146/annurev-cellbio-101011-155833

18. Kerstein PC, del Camino D, Moran MM, Stucky CL. Pharmacological blockade of TRPA1 inhibits mechanical firing in nociceptors. *Mol Pain*. 2009;5:19. doi:10.1186/1744-8069-5-19

19. Basbaum AI, Bautista DM, Scherrer G, Julius D. Cellular and molecular mechanisms of pain. *Cell*. 2009;139:267-284. doi:10.1016/j.cell.2009.09.028

20. Bennett DL, Clark AJ, Huang J, Waxman SG, Dib-hajj SD. The role of voltage-gated sodium channels in pain signaling. *Physiol Rev*. 2019;99:1079-1151. doi:10.1152/physrev.00052.2017

21. Chen L, Yang G, Grosser T. Prostanoids and inflammatory pain. *Prostaglandins Other Lipid Mediat*. 2013;104-105:58-66. doi:10.1016/j.prostaglandins.2012.08.006

22. Zhuo M. Ionotropic glutamate receptors contribute to pain transmission and chronic pain. *Neuropharmacology*. 2017;112:228-234. doi:10.1016/j.neuropharm.2016.08.014

23. Petrenko AB, Yamakura T, Baba H, Shimoji K. The role of N-methyl-D-aspartate (NMDA) receptors in pain: a review. *Anesth Analg*. 2003;97:1108-1116. doi:10.1213/01.ANE.0000081061.12235.55

24. Kieffer BL, Evans CJ. Opioid receptors: from binding sites to visible molecules in vivo. *Neuropharmacology*. 2009;56:205-212. doi:10.1016/j.neuropharm.2008.07.033

25. Labuz D, Mousa SA, Schäfer M, Stein C, Machelska H. Relative contribution of peripheral versus central opioid receptors to antinociception. *Brain Res*. 2007;1160:30-38. doi:10.1016/j.brainres.2007.05.049

26. Saxena AK, Jain PN, Bhatnagar S. The prevalence of chronic pain among adults in India. *Indian J Palliat Care*. 2018;24(4):472-477.

27. Nahin RL. Estimates of pain prevalence and severity in adults: United States, 2012. *J Pain*. 2015;16(8):769-780. doi:10.1016/j.jpain.2015.05.002

28. Breivik H, Collett B, Ventafridda V, Cohen R, Gallacher D. Survey of chronic pain in Europe: prevalence, impact on daily life, and treatment. *Eur J Pain*. 2006;10:287-333. doi:10.1016/j.ejpain.2005.06.009

29. Elzahaf RA, Tashani OA, Unsworth BA, Johnson MI. The prevalence of chronic pain with an analysis of countries with a Human Development Index less than 0.9: a

systematic review without meta-analysis. *Curr Med Res Opin*. 2012;28(7):1221-1229. doi:10.1185/03007995.2012.703132

30. Schopflocher D, Taenzer P, Jovey R. The prevalence of chronic pain in Canada. *Pain Res Manag*. 2011;16(6):445-450.

31. Von Korff M, Dunn KM. Chronic pain reconsidered. *Pain*. 2008;138(2):267-276. doi:10.1016/j.pain.2007.12.010.

32. Kamerman PR, Bradshaw D, Laubscher R, et al. Almost 1 in 5 South African adults have chronic pain: a prevalence study conducted in a large nationally representative sample. *Pain*. 2020;161(7):1629-1635.

33. de Souza JB, Grossmann E, Perissinotti DMN, De Oliveira Junior JO, da Fonseca PRB, De Paula Posso I. Prevalence of chronic pain, treatments, perception, and interference on life activities: Brazilian population-based survey. *Pain Res Manag*. 2017;2017:Article ID=4643830. doi:10.1155/2017/4643830

34. Kolodny A, Courtwright DT, Hwang CS, et al. The prescription opioid and heroin crisis: a public health approach to an epidemic of addiction. *Annu Rev Public Health*. 2015;36:559-574. doi:10.1146/annurev-publhealth-031914-122957

35. Craig BM, Strassels SA. Out-of-pocket prices of opioid analgesics in the United States, 1999–2004. *Pain Med*. 2010;11:240-247.

36. Dhalla IA, Persaud N, Juurlink DN. Facing up to the prescription opioid crisis. *BMJ*. 2011;343:d5142. doi:10.1136/bmj.d5142

37. Zylka MJ. Pain-relieving prospects for adenosine receptors and ectonucleotidases. *Trends Mol Med*. 2011;17(4):188-196. doi:10.1016/j.molmed.2010.12.006.

38. Chen Z, Janes K, Chen C, et al. Controlling murine and rat chronic pain through A_3 adenosine receptor activation. *FASEB J*. 2012;26:1855-1865. doi:10.1096/fj.11-201541

39. Godfrey L, Yan L, Clarke GD, Ledent C, Kitchen I, Hourani SMO. Modulation of paracetamol antinoiception by caffeine and by selective adenosine A_2 receptor antagonists in mice. *Eur J Pharmacol*. 2006;531:80-86. doi:10.1016/j.ejphar.2005.12.004

40. Savegnago L, Jesse CR, Nogueira CW. Caffeine and a selective adenosine A_{2B} receptor antagonist but not imidazoline receptor antagonists modulate antinociception induced by diphenyl diselenide in mice. *Neurosci Lett*. 2008;436:120-123. doi:10.1016/j.neulet.2008.03.003

41. Goldman N, Chen M, Fujita T, et al. Adenosine A_1 receptors mediate local anti-nociceptive effects of acupuncture. 2010;13(7):883-888. doi:10.1038/nn.2562

42. Little JW, Ford A, Symons-liguori AM, et al. Endogenous adenosine A_3 receptor activation selectively alleviates persistent pain states. *Brain*. 2015;138:28-35. doi:10.1093/brain/awu330

43. Borea PA, Gessi S, Merighi S, Vincenzi F, Varani K. Pharmacology of adenosine receptors: the state of the art. *Physiol Rev*. 2018;98:1591-1625. doi:10.1152/physrev.00049.2017

44. Fredholm BB, Ijzerman AP, Jacobson KA, Klotz K-N, Linden J. International Union of Pharmacology. XXV. Nomenclature and classification of adenosine receptors. *Pharmacol Rev*. 2001;53(4):527-552.

45. Fredholm BB, IJzerman AP, Jacobson KA, Linden J, Muller CE. International Union of Basic and Clinical Pharmacology. LXXXI. Nomenclature and classification of adenosine receptors—an update. *Pharmacol Rev*. 2011;63(1):1-34. doi:10.1124/pr.110.003285

46. Chen J, Eltzschig HK, Fredholm BB. Adenosine receptors as drug targets — what are the challenges? *Nat Rev Drug Discov*. 2013;12:265-286. doi:10.1038/nrd3955

47. Svenningsson P, Hall H, Sedvall G, Fredholm BB. Distribution of adenosine receptors in the postmortem human brain: an extended autoradiographic study. *Synapse*. 1997;27:322-335.

48. Bohm M, Pieske B, Ungerer M, Erdmann E. Characterization of A_1 adenosine receptors in atrial and ventricular myocardium from diseased human hearts. *Circ Res*. 1989;65(5):1201-1211.

49. Headrick JP, Peart JN, Reichelt ME, Haseler LJ. Adenosine and its receptors in the heart: regulation, retaliation and adaptation. *Biochim Biophys Acta*. 2011;1808:1413-1428. doi:10.1016/j.bbamem.2010.11.016

50. Modlinger PS, J WW. No Title. *Curr Opin Nephrol Hypertens*. 2003;12(5):497-502.

51. Yip L, Taylor C, Whiting CC, Fathman CG. Diminished adenosine A_1 receptor expression in pancreatic a-cells may contribute to the pathology of type 1 diabetes. *Diabetes*. 2013;62:4208-4219. doi:10.2337/db13-0614

52. Sawynok J. Adenosine receptor targets for pain. *Neuroscience*. 2016;338:1-18. doi:10.1016/j.neuroscience.2015.10.031

53. Vincenzi F, Targa M, Romagnoli R, et al. TRR469, a potent A_1 adenosine receptor allosteric modulator, exhibits anti-nociceptive properties in acute and neuropathic pain models in mice. *Neuropharmacology*. 2014;81:6-14. doi:10.1016/j.neuropharm.2014.01.028

54. Doyle TM, Largent-Milnes TM, Chen Z, et al. Chronic morphine-induced changes in signaling at the A_3 adenosine receptor contribute to morphine-induced hyperalgesia, tolerance, and withdrawal. *J Pharmacol Exp Ther*. 2020;374:331-341. doi:10.1124/jpet.120.000004

55. Sjolund K, von Heijne M, Hao J-X, Xu XJ, Sollevi A, Wisenfeld-Hallin Z. Intrathecal administration of the adenosine A_1 receptor agonist R-phenylisopropyl adenosine reduces

presumed pain behaviour in a rat model of central pain. *Neurosci Lett*. 1998;243:89-92.

56. Bastia E, Varani K, Monopoli A, Bertorelli R. Effects of A_1 and A_{2A} adenosine receptor ligands in mouse acute models of pain. *Neurosci Lett*. 2002;328:241-244.

57. Jacobson KA, Gao Z-G. Adenosine receptors as therapeutic targets. *Nat Rev Drug Discov*. 2006;5(3):247-264. doi:10.1038/nrd1983.Adenosine

58. Bailey A, Ledent C, Kelly M, Hourani SMO, Kitchen I. Changes in spinal delta and dappa opioid systems in mice deficient in the A_{2A} receptor gene. *J Neurosci*. 2002;22(21):9210-9220.

59. Sardi N, Tobaldini G, Morais R, Fischer L. Nucleus accumbens mediates the pronociceptive effect of sleep deprivation. *Pain*. 2018;159:75-84.

60. Kwilasz AJ, Ellis A, Wieseler J, et al. Sustained reversal of central neuropathic pain induced by a single intrathecal injection of adenosine A_{2A} receptor agonists. *Brain Behav Immun*. 2018;69:470-479. doi:10.1016/j.bbi.2018.01.005

61. Schindler CW, Karcz-kubicha M, Thorndike EB, et al. Role of central and peripheral adenosine receptors in the cardiovascular responses to intraperitoneal injections of adenosine A_1 and A_{2A} subtype receptor agonists. 2005:642-650. doi:10.1038/sj.bjp.0706043

62. Abo-salem OM, Hayallah AM, Bilkei-gorzo A, Filipek B, Zimmer A, Mu CE. Antinociceptive effects of novel A_{2B} adenosine receptor antagonists antinociceptive effects of novel A_{2B} adenosine receptor antagonists. 2004;(August 2016). doi:10.1124/jpet.103.056036

63. Hu X, Adebiyi MG, Luo J, et al. Sustained elevated adenosine via ADORA2B promotes chronic pain through neuro-immune interaction. *Cell Rep*. 2017;16(1):106-119. doi:10.1016/j.celrep.2016.05.080.Sustained

64. Dixon AK, Gubitz AK, Sirinathsinghji DJS, Richardson PJ, Freeman TC. Tissue distribution of adenosine receptor mRNAs in the rat. *Br J Pharmacol*. 1996;118:1461-1468.

65. Tosh DK, Padia J, Salvemini D, Jacobson KA. Efficient, large-scale synthesis and preclinical studies of MRS5698, a highly selective A_3 adenosine receptor agonist that protects against chronic neuropathic pain. *Purinergic Signal*. 2015;11:371-387. doi:10.1007/s11302-015-9459-2

66. Tosh DK, Paoletta S, Chen Z, et al. Structure-based design, synthesis by click chemistry and in vivo activity of highly selective A_3 adenosine receptor agonists. *Medchemcomm*. 2015;6:555-563. doi:10.1039/C4MD00571F.Structure-Based

67. Suresh RR, Jain S, Chen Z, et al. Design and in vivo activity of A_3 adenosine receptor agonist prodrugs. *Purinergic Signal*. 2020;16:367-377.

68. Ford A, Castonguay A, Cottet M, et al. Engagement of the GABA to KCC2 signaling pathway contributes to the analgesic effects of A_3AR agonists in neuropathic pain. *J Neurosci*. 2015;35(15):6057-6067. doi:10.1523/JNEUROSCI.4495-14.2015

69. Janes K, Esposito E, Doyle T, et al. A_3 adenosine receptor agonist prevents the development of paclitaxel-induced neuropathic pain by modulating spinal glial- restricted redox-dependent signaling pathways. *Pain*. 2014;155(12):2560-2567. doi:10.1016/j.pain.2014.09.016.A

70. Janes K, Symons-liguori AM, Jacobson KA, Salvemini D. Identification of A_3 adenosine receptor agonists as novel non-narcotic analgesics. *Br J Pharmacol*. 2016;173:1253-1267. doi:10.1111/bph.13446

71. Stoilov RM, Licheva RN, Mihaylova MK, et al. Therapeutic effect of oral CF101 in patients with rheumatoid arthritis: a double-blind, placebo-controlled phase II study. *Immunome Res*. 2014;11(1):article ID 1000087. doi:10.4172/17457580.1000087

72. Stemmer SM, Benjaminov O, Medalia G, et al. CF102 for thetreatment of hepatocellular Carcinoma: a phase I/II, open-label, dose-escalation study. *Oncologist*. 2013;18:25-26. doi:10.1634/theoncologist.2012–0211

73. David M, Akerman L, Ziv M, et al. Treatment of plaque-type psoriasis with oral CF101: data from an exploratory randomized phase 2 clinical trial. *J Eur Acad Dermatology Venereol*. 2012;26:361-367. doi:10.1111/j.1468-3083.2011.04078.x

74. Salehi B, Stojanovic-Radic Z, Mateji J, et al. The therapeutic potential of curcumin: a review of clinical trials. *Eur J Med Chem*. 2019;163:527-545. doi:10.1016/j.ejmech.2018.12.016

75. Kunnumakkara AB, Bordoloi D, Padmavathi G, et al. Curcumin, the golden nutraceutical: multitargeting for multiple chronic diseases. *Br J Pharmacol*. 2017;174:1325-1348. doi:10.1111/bph.13621

76. Xu X-Y, Meng X, Li S, Gan R-Y, Li Y, Li H-B. Bioactivity, health benefits, and related molecular mechanisms of curcumin: current progress, challenges, and perspectives. *Nutrients*. 2018;10:1553. doi:10.3390/nu10101553

77. Anand P, Kunnumakkara AB, Newman RA, Aggarwal BB. Bioavailability of curcumin: problems and promises. *Mol Pharm*. 2007;4(6):807-818. doi:10.1021/mp700113r

78. Rocks N, Bekaert S, Coia I, et al. Curcumin – cyclodextrin complexes potentiate gemcitabine effects in an orthotopic mouse model of lung cancer. *Br J Cancer*. 2012;107(August):1083-1092. doi:10.1038/bjc.2012.379

79. Chuang E, Lin K, Huang T, et al. An intestinal “Transformers ”-like nanocarrier system for enhancing the oral bioavailability of poorly water-soluble drugs. *ACS Nano*. 2018;12:6389-6397. doi:10.1021/acsnano.8b00470

80. Yallapu MM, Nagesh PKB, Jaggi M, Chauhan SC. Therapeutic applications of curcumin nanoformulations. *AAPS J*. 2015;17(6):1341-1356. doi:10.1208/s12248-015-9811-z

81. Bisht S, Khan MA, Bekhit M, et al. A polymeric nanoparticle formulation of curcumin (NanoCurc^{TM}) ameliorates CCl 4-induced hepatic injury and fibrosis through reduction of pro-inflammatory cytokines and stellate cell activation. *Lab Investig*. 2011;91(April):1383-1395. doi:10.1038/labinvest.2011.86

82. Ahmadi M, Hajialilo M, Dolati S, Fard SE. The effects of nanocurcumin on Treg cell responses and treatment of ankylosing spondylitis patients: a randomized, double-blind, placebo-controlled clinical trial. *J Cell Biochem*. 2020;121:103-110. doi:10.1002/jcb.28901

83. Agarwal KA, Tripathi CD, Agarwal BB, Saluja S. Efficacy of turmeric (curcumin) in pain and postoperative fatigue after laparoscopic cholecystectomy: a double-blind, randomized placebo-controlled study. *Surg Endosc*. 2011;25:3805-3810. doi:10.1007/s00464-011-1793-z

84. Zhu X, Li Q, Chang R, Yang D, Song Z, Guo Q. Curcumin alleviates neuropathic pain by inhibiting p300/CBP histone acetyltransferase activity-regulated expression of BDNF and COX-2 in a rat model. *PLoS One*. 2014;9(3):e91303. doi:10.1371/journal.pone.0091303

85. Yeon KY, Kim SA, Kim YH, et al. Curcumin produces an antihyperalgesic effect via antagonism of TRPV1. *J Dent Res*. 2009;89:170-174. doi:10.1177/0022034509356169

86. Glukhova A, Thal DM, Nguyen AT, et al. Structure of the adenosine A_1 receptor reveals the basis for subtype selectivity. *Cell*. 2017;168:867-877. doi:10.1016/j.cell.2017.01.042

87. Weinert T, Olieric N, Cheng R, et al. Serial millisecond crystallography for routine room-temperature structure determination at synchrotrons. *Nat Commun*. 2017;8:article number 542. doi:10.1038/s41467-017-00630-4

88. The Molecular Operating Environment (MOE). 2020. Chemical Computing Group Inc.; Montreal, Quebec, Canada.

89. The Protein Preparation Wizard, Maestro, MacroModel, and Glide, Schrodinger Release 2020-2. 2020.

90. Nabb DL, Song S, Kluthe KE, Daubert TA, Luedtke BE, Nuxoll AS. Polymicrobial interactions induce multidrug tolerance in *Staphylococcus aureus* through energy depletion. *Front Microbiol*. 2019;10:2803. doi:10.3389/fmicb.2019.02803

91. Rasband W. Image J. National Institutes of Health, Bethesda, Maryland, USA. https://imagej.nih.gov/ij/. Published 1997.

92. Hammond L. Measuring cell fluorescence using ImageJ. The Open Lab Book.

https://theolb.readthedocs.io/en/latest/imaging/measuring-cell-fluorescence-using-imagej.html. Published 2014.

93. Hunke M, Martinez W, Kashyap A, Bokoskie T, Pattabiraman M, Chandra S. Antineoplastic actions of cinnamic acids and their dimers in breast cancer cells: a comparative study. *Anticancer Res*. 2018;38:4469-4474. doi:10.21873/anticanres.12749

94. Stoddart LA, White CW, Nguyen K, Hill SJ, Pfleger KDG. Fluorescence-and bioluminescence-based approaches to study GPCR ligand binding. *Br J Pharmacol*. 2016;173:3028-3037. doi:10.1111/bph.13316

95. Almerico AM, Tutone M, Pantano L, Lauria A. A_3 adenosine receptor: homology modeling and 3D-QSAR studies. *J Mol Graph Model*. 2013;42:60-72. doi:10.1016/j.jmgm.2013.03.001

96. Thimm D, Schiedel AC, Sherbiny FF, et al. Ligand-specific binding and activation of the human adenosine A_{2B} receptor. *Biochemistry*. 2013;52:726-740. doi:10.1021/bi3012065

97. Müller CE, Jacobson KA. Recent developments in adenosine receptor ligands and their potential as novel drugs. *Biochim Biophys Acta*. 2011;1808(5):1290-1308. doi:10.1016/j.bbamem.2010.12.017

98. Klotz K-N. Adenosine receptors and their ligands. *Nauyn-Schmiedeberg's Arch Pharmacol*. 2000;362:382-391. doi:10.1007/s002100000315

99. Gao Z, Li Z, Baker SP, et al. Novel short-acting A2A adenosine receptor agonists for coronary vasodilation: inverse relationship between affinity and duration of action of A2A Agonists. *J Pharmacol Exp Ther*. 2001;298(1):209-218.

100. Cappellacci L, Franchetti P, Vita P, et al. 5'-Carbamoyl derivatives of 2'-C-methyl-purine nucleosides as selective A_1 adenosine receptor agonists: affinity, efficacy, and selectivity for A_1 receptor from different species. *Bioorg Med Chem*. 2008;16:336-353. doi:10.1016/j.bmc.2007.09.035

101. Jacobson KA, IJzerman AP, Linden J. 1, 3-dialkylxanthine derivatives having high potency as antagonists at human A_{2B} adenosine receptors. *Drug Dev Res*. 1999;47:45-53.

102. Prystowsky EN, Niazi I, Curtis AB, et al. Termination of paroxysmal supraventricular tachycardia by tecadenoson (CVT-510), a novel A_1-adenosine receptor agonist. *J Am Coll Cardiol*. 2003;42(6):1098-1102. doi:10.1016/S0735-1097(03)00987-2

103. Huang Z, Qu W, Eguchi N, et al. Adenosine A_{2A}, but not A_1, receptors mediate the arousal effect of caffeine. *Nat Neurosci*. 2005;8(7):858-859. doi:10.1038/nn1491

104. Draper-Joyce CJ, Khoshouei M, Thal DM, et al. Structure of the adenosine-bound human adenosine A_1 receptor–Gi complex. *Nature*. 2018;558:559-563. doi:10.1038/s41586-018-0236-6

105. Trzaskowski B, Latek D, Yuan S, Ghoshdastider U, Debinski A, Filipek S. Action of molecular switches in GPCRs- theoretical and experimental studies. *Curr Med Chem*. 2012;19:1090-1109.

106. Holst B, Nygaard R, Valentin-hansen L, et al. A conserved aromatic lock for the tryptophan rotameric switch in TM-VI of seven-transmembrane receptors. *J Biol Chem*. 2010;285(6):3973-3985. doi:10.1074/jbc.M109.064725

107. Fredholm BB, Irenius E, Kull B, Schulte G. Comparison of the potency of adenosine as an agonist at human adenosine receptors expressed in Chinese hamster ovary cells. *Biochem Pharmacol*. 2001;61:443-448.

108. Haroyan A, Mukuchyan V, Mkrtchyan N, et al. Efficacy and safety of curcumin and its combination with boswellic acid in osteoarthritis: a comparative, randomized, double-blind, placebo-controlled study. *BMC Complement Altern Med*. 2018;18:7. doi:10.1186/s12906-017-2062-z

109. Shep D, Khanwelkar C, Gade P, Karad S. Safety and efficacy of curcumin versus diclofenac in knee osteoarthritis: a randomized open-label parallel-arm study. *Trials*. 2019;20:214. doi:10.1186/s13063-019-3327-2

110. Sanmukhani J, Satodia V, Trivedi J, et al. Efficacy and safety of curcumin in major depressive disorder: a randomized controlled trial. *Phyther Res*. 2014;28:579-585. doi:10.1002/ptr.5025

111. Cheng A-L, Hsu C-H, Lin J-K, et al. Phase I clinical trial of curcumin, a chemopreventive agent, in patient with high-risk or pre-malignant lesions. *Anticancer Res*. 2001;21:2895-2900.

112. Nakamura M, Chi Y-M, Yan W-M, et al. Structure-Antinociceptive activity studies of incarvillateine, a monoterpene alkaloid from *Incarvillea sinensis*. *Planta Med*. 2001;67:114-117.

113. Premkumar LS. Transient receptor potential channels as rargets for phytochemicals. *ACS Chem Neurosci*. 2014;5:1117-1130. doi:10.1021/cn500094a

114. Yang F, Xiao X, Cheng W, et al. Structural mechanism underlying capsaicin binding and activation of TRPV1 ion channel. *Nat Chem Biol*. 2015;11(7):518-524. doi:10.1038/nchembio.1835

115. Caterina MJ, Schumacher MA, Tominaga M, Rosen TA, Levine JD, Julius D. The capsaicin receptor: a heat-activated ion channel in the pain pathway. *Nature*. 1997;389:816-824.

116. Riera C, Menozzi-Smarrito C, Affolter M, et al. Compounds from Sichuan and Melegueta peppers activate, covalently and non-covalently, TRPA1 and TRPV1 channels. *Br J Pharmacol*. 2009;157:1398-1409.

117. Abbas M. Modulation of TRPV1 channel function by natural products in the

treatment of pain. *Chem Biol Interact*. 2020;330:article number 109178.

118. Akula KK, Kulkarni SK. Effect of curcumin against pentylenetetrazol-induced seizure threshold in mice: possible involvement of adenosine A_1 receptors. *Phyther Res*. 2014;28:714-721.

119. Tendera M, Gaszewska-Zurek E, Parma Z, et al. The new oral adenosine A_1 receptor agonist capadenoson in male patients with stable angina. *Clin Res Cardiol*. 2012;101:585-591. doi:10.1007/s00392-012-0430-8

120. da Silva JS, Gabriel-Costa D, Sudo RT, et al. Adenosine A_{2A} receptor agonist prevents cardiac remodeling and dysfunction in spontaneously hypertensive male rats after myocardial infarction. *Drug Des Dev Ther*. 2017;11:553-562.

121. Johnston-Cox H, Koupenova M, Yang D, et al. The A_{2B} adenosine receptor modulates glucose homeostasis and obesity. *PLoS One*. 2012;7(7):e40584. doi:10.1371/journal.pone.0040584

122. Fishman P, Bar-yehuda S, Liang BT, Jacobson KA. Pharmacological and therapeutic effects of A_3 adenosine receptor agonists. *Drug Discov Today*. 2012;17(7/8):359-366. doi:10.1016/j.drudis.2011.10.007

123. Jacobson KA, Merighi S, Varani K, et al. A_3 adenosine receptors as modulators of inflammation: from medicinal chemistry to therapy. *Med Res Rev*. 2018;38(February 2017):1031-1072. doi:10.1002/med.21456

124. Schaddelee MP, Collins SD, Dejongh J, Boer AG De, Ijzerman AP, Danhof M. Pharmacokinetic/ pharmacodynamic modelling of the anti-hyperalgesic and anti-nociceptive effect of adenosine A_1 receptor partial agonists in neuropathic pain. *Eur J Pharmacol*. 2005;514:131-140. doi:10.1016/j.ejphar.2005.03.026